Published in final edited form as:
Eur J Nucl Med Mol Imaging. 2012 January ; 39(1): 165–181. doi:10.1007/s00259-011-1925-7.

Emerging roles for integrated imaging modalities in cardiovascular cell-based therapeutics: a clinical perspective

Peter J. Psaltis, **Robert D. Simari**, and **Martin Rodriguez-Porcel**
Division of Cardiovascular Diseases, Department of Internal Medicine, Mayo Clinic, 200 First St SW, Rochester, MN 55905, USA

Martin Rodriguez-Porcel: rodriguez.m@mayo.edu

Abstract

Despite preclinical promise, the progress of cell-based therapy to clinical cardiovascular practice has been slowed by several challenges and uncertainties that have been highlighted by the conflicting results of human trials. Most telling has been the revelation that current strategies fall short of achieving sufficient retention and engraftment of cells to meet the ambitious objective of myocardial regeneration. This has sparked novel research into the refinement of cell biology and delivery to overcome these shortcomings. Within this context, molecular imaging has emerged as a valuable tool for providing noninvasive surveillance of cell fate in vivo. Direct and indirect labelling of cells can be coupled with clinically relevant imaging modalities, such as radionuclide single photon emission computed tomography and positron emission tomography, and magnetic resonance imaging, to assess their short- and long-term distributions, along with their viability, proliferation and functional interaction with the host myocardium. This review details the strengths and limitations of the different cell labelling and imaging techniques and their potential application to the clinical realm. We also consider the broader, multifaceted utility of imaging throughout the cell therapy process, providing a discussion of its considerable value during cell delivery and its importance during the evaluation of cardiac outcomes in clinical studies.

Keywords

Stem cells; Imaging; Heart; Magnetic resonance imaging; Single photon emission computed tomography; Positron emission tomography; Tracking; Delivery

Introduction

Over the last decade, the use of progenitor cell therapies has emerged as an exciting option for the treatment of a range of cardiovascular diseases [1]. Preclinical small and large animal experiments have demonstrated that a diverse array of mature and immature cell types may confer benefit to myocardial function and perfusion after cardiac injury. This promise has translated into a steady stream of clinical research, beginning with early proof of principle studies [2, 3] and evolving to multicentre, placebo-controlled, randomised trials that are actively recruiting patients today. Several thousand individuals have now received unfractionated bone marrow cells (BMCs) [4–8], skeletal myoblasts (SkMs) [9], mesenchymal stromal/stem cells (MSCs) [10] or pro-angiogenic, endothelial progenitor cells

Correspondence to: Martin Rodriguez-Porcel, rodriguez.m@mayo.edu.

Conflicts of interest None.

(EPCs) [11] in studies investigating cellular treatment for acute and chronic myocardial infarction (MI), non-revascularisable ischaemic heart disease (IHD) and ischaemic and nonischaemic cardiomyopathy (NICM). Meta-analyses have concluded that cellular treatment for MI may lead to modest augmentation of left ventricular (LV) systolic function compared to controls (approximately 3% for absolute ejection fraction) [12, 13]. However, when analysed individually, trial results have been inconsistent [6, 14, 15]. Such discrepant observations are largely attributable to a lack of standardisation in the methodology employed by different investigative groups, relating to a variety of critical considerations, which can be divided into: (1) patient recruitment criteria, (2) cell product (type, preparation and dose), (3) timing and route of cell delivery, and (4) assessment of endpoints [16, 17].

As research efforts continue to address the biological limitations of different cell types, an important role has emerged for cardiac, cellular and molecular imaging to bring greater understanding and optimisation of the mechanics of cell delivery, the short- and long-term fate of implanted cells and their interactions with the host myocardium, as important interim outcomes after cell transfer. Here, we discuss the current and future utility of imaging as it relates to various key stages of the cell therapy process, focusing on image-based navigation of cell delivery to the myocardium and the noninvasive tracking of cell fate after administration, using clinically applicable strategies. Emphasis will be on the lessons learned from previous studies and where the focus should be placed in the future.

Imaging to assist cell delivery

A fundamental requirement of successful myocardial salvage is that sufficient viable cells reach their target sites soon after administration and are retained there to enable their long-term survival, engraftment, proliferation and function. Exogenous cells can be directed to the heart (1) systemically by peripheral venous injection, (2) regionally, by coronary arterial or venous infusion or (3) locally, by direct transepicardial, transendocardial or intrapericardial implantation. The choice of delivery method is likely influenced by the underlying disease process and cell type to be used, along with the expertise and resources of individual research groups. However, almost uniformly, studies have shown low rates of cell retention and engraftment across cell types, delivery methods and myocardial disease substrates, restricting the scope of benefit that can be achieved with current cell therapy strategies [18, 19].

By virtue of its practicality, safety and cost, fluoroscopically guided intracoronary infusion has been the commonest method used in clinical studies of cell therapy [6, 8, 14, 20], with the potential of cell distribution in the affected coronary artery territory. However, this approach may not be feasible in the setting of totally occluded coronary arteries and is hindered by direct washout of cells limiting first-pass retention and by the deleterious aggregation of adherent or large-sized cells (e.g. MSCs) within the coronary microvasculature [21–23]. Delivery by intramyocardial injection, either by open transepicardial or percutaneous, catheter-based transendocardial approach (Fig. 1a, b), targets specific areas of myocardium more directly. Although still hampered by significant early injectate loss [24], a direct injection approach appears to have advantages over systemic and intracoronary delivery with respect to cardiac cell retention [18], non-cardiac cell entrapment [22] and overall therapeutic effect [17, 25]. Cell retention and myocardial distribution are similar between the transendocardial and transepicardial strategies [26], although catheter-based injection is less invasive, increasing its broader clinical applicability and potentially making it amenable to repeated cell interventions [27]. It is in this context of transendocardial delivery, more so than for other delivery routes, that an important role has emerged for adjuvant imaging to guide the location of injection sites and determine the success of cell implantation in the myocardium [28].

Adjuvant imaging during catheter-based cell delivery

Most available injection catheter systems have been used with traditional biplanar X-ray fluoroscopy to visualise catheter manipulation and placement inside the LV cavity [24, 29–32] (Fig. 1c). This may be further assisted by pre-procedural imaging and planning with complementary modalities [e.g. echocardiography, single photon emission computed tomography (SPECT), positron emission tomography (PET) and magnetic resonance imaging (MRI)] to facilitate the selection of ischaemic or dysfunctional myocardial regions for cell delivery. Alternatively catheters have also been designed with sensor technology to allow their detection and navigation in real time with enhanced three-dimensional (3-D) precision. The most widely applied example of this is the MyoStar™ catheter (Fig. 1b) which is used in conjunction with the NOGA® XP Cardiac Navigation System (Biologics Delivery Systems Group, Cordis Corporation, Diamond Bar, CA, USA) [33].

NOGA® XP is a non-fluoroscopic, magnetic, electromechanical guidance technology that combines ultralow magnetic field sources (5×10^{-5} to 5×10^{-6} T) and location sensor-tipped catheter electrodes to accurately and reproducibly track a catheter's trajectory inside the LV to within 1-mm distances. As endocardial sites are contacted and "sampled" by the mapping catheter, spatial, electrophysiological and mechanical data are acquired in real time to create 3-D, colour-coded reconstructions of the endoventricular surface. Electrical voltage amplitudes and mechanical contractility assessment (expressed as linear local shortening ratio) are used in combination to identify regional impairment of myocardial function, perfusion and/or viability. This enables the detection of non-viable scar and peri-infarct tissue in MI [34] (Fig. 1d, e), hibernating myocardium in chronic IHD and ischaemic cardiomyopathy [35, 36] and segmental fibrosis in NICM [37]. In turn, this information can be used to direct focused selection of target sites for cell delivery, with 3-D visualisation of injection density and distribution. Electromechanical navigation has thus been able to guide implantation of various cell types in large animal and clinical studies of chronic IHD [11, 38], acute MI [39] and most recently NICM [40]. It has also been used during follow-up to assess for improvement in regional electromechanical function after cell therapy, although this application has not been strictly validated [38, 41]. Over 50 clinical NOGA® XP systems are currently in use [28]. Barriers to wider application include high cost and demand on operator expertise, training and accreditation [42]. Ongoing upgrades are designed to advance the technology by reducing mapping artefacts, shortening catheter response times, improving data accuracy and image quality and enabling stereotactic use [43, 44]. Non-contact electromechanical navigation is also under investigation for cell delivery, using the Endocardial Solutions (ESI)™ mapping system [45].

One shortcoming of catheter-based electromechanical mapping is its imperfect accuracy for sizing territories of ischaemia, infarction and fibrosis in the presence of severe LV dilatation [33]. Although more investigative, other catheter systems have undergone modifications to allow their coupling with real-time MR fluoroscopy (e.g. Stiletto™ [46] and MyoCath™ [47] catheters) and high-resolution 3-D echocardiography [48, 49]. MRI provides excellent 3-D anatomical and functional definition of the heart, along with high-resolution depiction and quantification of myocardial fibrosis and perfusion in both ischaemic and nonischaemic cardiac pathologies. The advent of ultrafast MRI technology and later generation, interactive scanners has opened up numerous possibilities for real-time MR fluoroscopy to be applied in interventional cardiovascular practice including the targeted delivery of endovascular and intramyocardial injectates (e.g. cells, genes, drugs) [50, 51]. Various scanning systems have been created for MRI-based interventions, including the hybrid XMR system which integrates real-time X-ray and non-ionising MR fluoroscopy for flexible, complementary imaging [52, 53]. Visualisation of catheters can be achieved by passive or active tracking [50]. Passive devices are detected on MR images as a signal void or susceptibility artefact, which can be enhanced by coating the catheter shaft or tip with paramagnetic markers (e.g.

dysprosium oxide, gadolinium oxide, ferrite admixtures) and by administering blood pool contrast medium. An advantage of this type of tracking is that it can be performed with conventional MR scanners, without adjustments to hardware or software or the need for image post-processing. However, these catheters are prone to safety hazards during MR fluoroscopy due to ferromagnetic attractive forces or overheating during radiofrequency transmission [54]. By comparison, active tracking requires catheters to be equipped with receiving microcoils along their shaft and/or tip that interface with the MRI scanner to provide signals within the native anatomy. This usually necessitates specialised hardware and post-processing technology to superimpose the image of the coil on the road map image of the heart. Such catheters have been used to perform MRI-guided intramyocardial injections in large animal studies with good precision and safety [46, 55, 56] (Fig. 1f–h).

Despite the promise of initial preclinical validation, there has been limited ongoing research or manufacturing interest to develop US Food and Drug Administration (FDA)-approved, MRI-compatible catheters for transendocardial intervention. Concerns also surround the ability to monitor acute cardiac patients in a high magnetic field environment during invasive procedures, and additional expertise would be required for the interventional cardiologist to interpret the graphical interfaces during real-time MRI acquisition. In the short term, the role for cardiac MRI during cell delivery is therefore likely to be as an adjunct to other types of navigation imaging. Custom-made software may allow previously acquired MR images to be merged with real-time X-ray fluoroscopy [57] or electromechanical mapping [58]. This practice of bimodal imaging enhances 3-D anatomical and tissue characterisation so that injections can be avoided in areas of thinned or non-viable myocardium.

In summary, biplanar X-ray fluoroscopy and electromechanical mapping currently remain the most established tools for guiding transendocardial cell delivery and have been utilised in a variety of completed clinical studies (Table 1), as well as numerous ones that are ongoing (www.clinicaltrials.gov). Technical modifications and the integration of adjuvant imaging modalities are expected to further strengthen the role of real-time imaging in navigated cell delivery. It is also likely that imaging will facilitate the emergence of new approaches to cell delivery, such as percutaneous intrapericardial injection, which has recently been performed in pigs under guidance by X-ray fluoroscopy together with intravascular ultrasound [59] or MRI [60].

Imaging to assess cell fate

The ability to accurately trace cell fate is of utmost importance if key questions are to be addressed regarding optimal cell type and dose, efficiency of cell delivery, cell biodistribution and engraftment and the mechanisms by which cells may impart myocardial restoration (differentiation versus paracrine effects). Noninvasive tracking is therefore necessary to temporally monitor the presence of cells in intact subjects and to elucidate their kinetics and biological interactions with recipient myocardium over time.

In order to be visually distinguishable from endogenous tissue, exogenous cells must first be labelled (for direct or indirect monitoring) prior to their administration. Ideally, techniques used for cell labelling and imaging should be non-toxic to both the cells and the recipient organ(s) and possess a good balance of spatial resolution and cell detection sensitivity. Furthermore, they should have low enough radiation and contrast exposure to enable serial monitoring at multiple time points, high specificity so that signal can be interpreted as coming exclusively from viable, labelled cells and good quantitative accuracy to provide a reproducible measure of actual cell numbers.

Focusing on clinically translatable modalities, cell labelling is usually performed either (1) directly, which is best suited to the assessment of short-term retention and distribution of cells or (2) indirectly by reporter gene transfer, which may enable longer-term monitoring of cell engraftment, viability and interaction with the myocardium (Fig. 2).

Assessment of short-term cell fate

The most commonly used approach to label cells directly is by incubating them in vitro with magnetic contrast agents for MRI surveillance [61, 62] or radionuclide agents for detection with SPECT [63–66] or PET [19, 67, 68].

Magnetic resonance imaging—Cardiac MRI has several qualities that make it a good candidate for serial imaging of individual subjects, as required during longitudinal assessment of cell therapy efficacy [69]. In what relates to the monitoring of administered cells, direct labelling for MRI has been mostly achieved with magnetic nanoparticles (MNP), which are typically superparamagnetic but can also be synthesised to be ferromagnetic or paramagnetic. Superparamagnetic MNP induce strong magnetic field disturbances that reduce T2* relaxation time and create hypointense signal voids on T2- and T2*-weighted images. They are usually composed of an iron oxide core (magnetite and/or maghemite) measuring 3–5 mm in diameter, with a polymeric or polysaccharide coating (e.g. dextran), which maintains their solubility and reduces their agglomeration. This structure renders them biodegradable via iron metabolic pathways and largely biocompatible. With physical and chemical modifications, several generations of MNP have now been synthesised. Early generation MNP comprised superparamagnetic iron oxide particles (SPIO, 60–150 nm in diameter), such as the ferumoxide, Feridex (Advanced Magnetics, Cambridge, MA, USA) and micron-sized iron oxide particles (MPIO, 0.7–1.6 μm) [70]. SPIO contain relatively thin dextran coats and tend to form polycrystalline clusters, allowing their rapid clearance from the circulation by the reticuloendothelial system. Subsequently smaller MNP have been developed, including citrate-coated ultra small paramagnetic iron oxides (USPIO, 10–40 nm) and monocrystalline iron oxide nanoparticles (MION 10–30 nm). As a result of their extensive polymer coating, these nano-sized MNP remain monodisperse in solution, with longer circulatory half-lives. They also have higher relaxivities than first-generation MNP, allowing deeper penetration into tissue spaces and conferring higher sensitivity. Highly stable, cross-linked derivatives of MION, known as CLIO, have become particularly attractive for targeted molecular imaging [71] and can be conjugated to fluorochromes (e.g. rhodamine B isothiocyanate) for multimodal detection by MRI and optical imaging techniques [72].

Iron oxide-labelled cells have been successfully imaged in both small [73–75] and large animal cardiac models [61, 76, 77] using clinical MR scanners (1.5–3 T). In this context, transplanted cells ($\geq 10^5$ cells) have been visualised in the initial hours to days after implantation, providing verification of the success of their delivery and their precise location in the myocardium (e.g. relative to tissue scar). Cells on biomaterial scaffolds, a subject of continued investigation to enhance engraftment in recipient myocardium, have also been imaged [78, 79]. Although SPIO-based labelling has regulatory approval for the imaging of liver tumours [80] and lymph node metastases [81], the cessation of ferumoxide production in the USA and Europe poses a setback to clinical translation. As such, MRI tracking of cell therapy has not yet been adopted in human studies of cardiovascular disease, although there are encouraging precedents for its use in patients with melanoma [82] and brain trauma [83].

Despite their practical simplicity, iron oxide nanoparticles have several shortcomings including their potential for cytotoxicity [84]. Although they do not appear to negatively effect cell viability or proliferation at the concentrations required for cardiac MRI [85, 86],

impairment of other cellular properties has been documented, including reduced migration of EPCs [87] and diminished colony formation, migration and chondrogenic differentiation of MSCs [88, 89]. Like all direct labels, iron oxides also have limited utility for long-term tracking as they are not self-replicable and become diluted after cell fragmentation, fusion, division or migration [90]. Moreover, their physical detachment after cell death and subsequent ingestion by tissue-resident macrophages can result in persistent, nonspecific signal that may be misinterpreted as cell engraftment [75, 84, 91]. Quantification of cell number can also be hindered by the "blooming effect" of iron oxides and by signal void confounders such as myocardial haemorrhage or microvascular obstruction after MI [92]. Positive contrast techniques, specialised imaging sequences and post-processing methods may overcome some of these limitations [93, 94]. Alternative approaches are to use hyperintense signals on T1-weighted images to track cells labelled with paramagnetic contrast agents, such as manganese chloride compounds, traditional gadolinium chelates, or novel, high-sensitivity compounds which may have better safety profiles (e.g. gadolinium-containing carbon nanocapsules [95], gadofluorine M-Cy3 [96]). Cell tracking has also been performed using non-proton fluorine MRI (^{19}F-MRI), which has a higher signal to noise ratio compared to standard proton-based MRI, allowing it to sensitively detect perfluorocarbon-labelled cells as "hot" spots [97]. Although experimental at present, many of these advances in MRI tracking may be translatable to clinical studies in the future.

Radionuclide imaging—Direct labelling for cell tracking by SPECT or PET can be performed by incubating cells with radioactive tracers, many of which are already in clinical use. Examples include ^{111}In-oxine and ^{99m}Tc-hexamethylpropylenamineoxine (HMPAO) for SPECT and ^{18}F-fluorodeoxyglucose (FDG) and ^{64}Cu-pyruvaldehyde-bis(*N*4-methylthiosemicarbazone) (PTSM) for PET. Cell detection sensitivity is higher with PET (femtomolar) and SPECT (nanomolar) compared to MRI (micromolar). This advantage is offset by their exposure to ionising radiation, as well as their lower spatial resolution (millimetres compared to micrometres for MRI), which limits the anatomical detail with which cells can be localised to the myocardium. However, this can be improved by performing hybrid imaging whereby radionuclide images are integrated with those from computed tomography (CT) or MRI [26, 98]. PET, in particular, allows accurate quantification of cell number by measuring retention as a percentage of total injected dose [99]. As opposed to PET, SPECT-based cell labelling is able to detect simultaneous signals of different energies (80–250 keV) by varying the detection windows, enabling its dual-purpose application for cell tracking concurrent with ^{201}Tl- or ^{99m}Tc-based perfusion imaging.

The physical half-lives of radiotracers partly determine the length of follow-up possible. In the case of ^{18}F-FDG (half-life of 109 min), monitoring is generally focused to the first few hours after cell delivery [67], although this may be extended with higher sensitivity scanners (e.g. LSO and GSO detectors). Surveillance for a few days is possible with PET-based tracking of ^{64}Cu- PTSM (half-life of 12 h) and SPECT imaging of ^{111}In compounds (half-life of 2.8 days). Long-term monitoring of radiolabelled cells is also prevented by the aforementioned, inherent limitations of direct labelling that result in signal dilution over time. Biological half-life, labelling efficiency and cytotoxicity are all important considerations when applying different radionuclide labels to specific cell types. For example, cell uptake of ^{111}In compounds is modest and their emission of high-energy electrons has resulted in cytotoxic effects, such as reduced viability and colony-forming ability of haematopoietic progenitor cells [100, 101] and compromised viability, proliferation, migratory capacity and metabolic integrity of MSCs [102–104]. Better cell tolerability has been shown with the PET tracer ^{64}Cu-PTSM [105].

Cell imaging with SPECT or PET has been implemented in a number of preclinical studies to address key questions concerning the efficiency of cell retention for different cell types and delivery techniques [18, 26, 68, 106, 107]. Early rodent studies shed light on the initial homing of cells to the infarcted myocardium after systemic delivery and the temporal profile of their distribution to the lungs followed by the liver, kidneys and spleen [100, 106]. In large animal studies of MI, radionuclide tracking has been used to demonstrate better myocardial retention of cells, with less pulmonary entrapment, after direct intramyocardial implantation compared to peripheral or coronary vascular infusion [18, 63]. Recently, serial SPECT/CT imaging was used to show that retention rates were similar between surgical transepicardial and percutaneous transendocardial injection of ^{111}In-tropolone-labelled EPCs in dogs [26]. Valuable lessons were also learned from a study in which ^{18}F-FDG-labelled cells were imaged with dynamic PET/ CT to compare two different strategies of intracoronary infusion [68]. After cell delivery with repeated cycles of the stop-flow infusion technique (common in many clinical trials), myocardial ^{18}F-FDG signal (as a surrogate for the presence of cells) was transiently higher during balloon occlusion, before falling sharply during balloon deflation. In contrast, first-pass clearance of cells was observed to be more gradual, with higher resultant myocardial retention, when cells were delivered as a single, high-concentration bolus.

Unlike MRI, radionuclide detection of directly labelled cells has also been applied in the realm of clinical cardiovascular studies (Table 2). Hofmann et al. described a small series of MI patients, in whom 3-D PET imaging was performed within 90 min after intracoronary or intravenous infusion of ^{18}F-FDG-labelled cells (unselected BMCs or CD34-enriched cells) [19]. Cardiac cell signal was not observed after systemic administration of unselected cells, but was present at very low levels (1.3–2.6%) in the infarct and border regions after intracoronary delivery. Retention was augmented considerably for $CD34^+$ cells which distributed selectively to the border zone (14–39%). Similar data have been reported by other radionuclide studies in patients with acute or chronic MI [64, 66, 67, 108]. Further insights were also obtained from a study in which SPECT was used to monitor the retention of ^{111}In-labelled pro-angiogenic cells after intracoronary injection in patients with different aged infarcts [109]. Cardiac signal activity was highly variable, averaging 6.9% (range 1–19%) 1 h after cell transfer, before declining to 2% after 3–4 days. Retention was highest in patients with recent MI (<14 days old), progressively diminishing in those with intermediate (up to 1 year old) or chronic (>1 year) infarcts.

By consistently revealing the modest extent to which cells are retained in the heart, as well as their distribution to other organs, the above-mentioned tracking studies have stimulated vigorous research to optimise cell delivery and biology in order to improve cell engraftment and treatment outcomes [99, 110]. Their findings also provide useful context to help contemplate the inconsistencies between clinical trial results, the merits of systemic cell delivery [10] and the relative value of using unfractionated BMCs [6, 14], compared to enriched cell populations [11]. These studies also highlight the individual variability of cell therapy responses and the need for future treatment regimes to be carefully tailored to each patient.

Assessment of long-term cell fate

After successful delivery and early retention of cells in the heart, it is desirable to monitor their long-term survival and functionality, which may be achieved by indirect cell labelling using reporter gene transfer. In this imaging strategy, cells are engineered to produce a non-native or overexpressed enzyme, receptor or protein and when this protein interacts with an exogenously given substrate it results in signal that can be used to distinguish implanted cells from endogenous cells with high specificity. Unlike direct labelling techniques, the

signal from reporter gene labels is only produced by viable cells with intact metabolic and synthetic function. Moreover, when the transgene has been permanently incorporated into the genomic DNA (i.e. stable transfection, as with retroviral or lentiviral vectors), it is passed on to daughter cell progeny during cell replication, avoiding signal dilution due to cell division. Reporter gene labelling is perhaps most attractive for highly proliferative cells (e.g. embryonic stem cells [111] and induced pluripotent stem cells [112]) where relatively few cells require transfection before clonal expansion.

Thus far, reporter gene strategies to track stem cell survival have been mainly based on optical bioluminescence imaging (BLI) using luciferase reporter genes (e.g. firefly luciferase, *Renilla* luciferase) in small animal studies [84, 111, 113, 114]. Expression of these enzymes allows the cells to oxidise specific probes (e.g. D-luciferin, coelenterazine), resulting in their emission of light photons, which can be detected by ultrasensitive charge-coupled device (CCD) cameras. Despite its many advantages for cell tracking in rodents (low cost, non-toxicity, high sensitivity), BLI suffers from low spatial resolution and a lack of tissue depth penetration, precluding its use in human subjects. However, reporter genes can also be adapted to clinical imaging modalities, most notably PET [115], but also SPECT [116] and MRI [117, 118].

Previous publications have described in detail the different types of reporter genes available for radionuclide detection [119–121]. In brief, these are based on either (1) intracellular enzymes which can trap the probe (e.g. herpes simplex virus thymidine kinase, HSV-tk) [111, 122], (2) cell membrane transporter proteins which enable probe uptake (e.g. sodium-iodide symporter, NIS) [116, 123] or (3) cell membrane receptors which bind directly to the probe (e.g. mutant dopamine D_2 receptors) [124]. Compared to SPECT, PET has significant flexibility for the production of specific probes to detect different processes (reporter genes in this case) in the living subject, allowing researchers to first identify the molecule to be imaged and then design a specific probe that will target that molecule. On the other side, SPECT imaging provides the possibility to investigate more than one signal simultaneously.

In vivo applications have also been described using reporter genes specially designed for targeted molecular MRI [117, 118]. These are based on the production of various proteins, such as enzymes that block water (proton) exchange, surface receptors that bind MR contrast agents or intracellular metalloproteins involved with iron metabolism (ferritin, transferrin receptor, tyrosinase) [117, 118, 125]. The ferritin gene is especially attractive as it greatly facilitates intracellular sequestration of iron (Fe^{3+}) resulting in T2/T2* shortening without the need for concomitant exogenous contrast agents. However, despite initial enthusiasm, MR imaging of reporter gene activity is hindered by higher background signal and lower sensitivity compared to radionuclide modalities and thus is not widely available or feasible for clinical translation in the foreseeable future.

So far, reporter gene monitoring has been performed predominantly in rodent models of cardiovascular disease [112, 115] and experience in large animal studies has been relatively limited [122, 126, 127]. In a porcine model of MI, in vivo and ex vivo techniques were used to track MSCs that had been labelled with triple fusion reporter genes [*Renilla* luciferase, red fluorescence protein (RFP), herpes simplex truncated thymidine kinase] and delivered by NOGA-guided transendocardial injection [122]. Engraftment of cells was detected by ^{18}F-FHBG PET and their localisation was verified by fusing these images with CT or MRI. Hybrid images revealed diffuse myocardial distribution of cells in the early stages after focal injection, with diminution of cardiac signal and uptake in other tissues after 7 days. This elegantly demonstrated that viable cells continue to be lost from the myocardium after their initial retention, probably through both lymphatic and circulatory migration to other organs. In another recent porcine study, PET/CT imaging demonstrated the value of

using bioscaf-folds to enhance retention of human MSCs that had been adenovirally transfected with *HSV1-sr39tk* [127]. At this stage, there is only one non-cardiac clinical report for reporter gene imaging of cells, in which PET was used to monitor *HSV1-tk* transfected cytolytic T cells in a patient with glioma [128].

Although reporter gene tracking offers a promising strategy for the long-term assessment of cellular engraftment, uncertainties remain relating to the safety of different viral vectors, the deleterious effects of genetic modification on cell integrity and function, the possibility of non-integrative (episomal) gene transfer resulting in unreliable or temporary signal and the diminution of transgene expression over time.

Multimodal cell tracking

Selection of the most appropriate labelling-imaging combination requires careful consideration of the respective advantages and disadvantages of each strategy (Table 3) and its ability to address the specific question in mind. It is also evident that in order to achieve comprehensive assessment of both short- and long-term cell fate, a multimodal or hybrid approach to cell tracking may be helpful, by integrating different techniques with complementary strengths [129, 130]. In terms of imaging modality, the higher spatial resolution of MRI is well suited to localising cell distribution in the myocardium, whereas the superior sensitivity and quantitative capabilities of radionuclide techniques (PET or SPECT) are more useful for determining cell number. As discussed before, reporter gene tracking is currently most advanced with PET and SPECT, thereby providing the best option for the long-term study of cell biology and fate. Fusion of PET or SPECT images with higher resolution spatial techniques (e.g. CT, MRI) has enabled radionuclide cell signals to be interpreted more precisely in their anatomical context [122]. Although this can be achieved by offline coregistration using fiducial markers in the field of view and specialised shape/pattern recognition software [131, 132], coregistration may be affected by differences in slice thickness between the modalities (e.g. PET, CT) and movement of the patient (or organ), while signal resolution may also be dependent on the size of markers. These issues are more avoidable with clinically available, integrated, hybrid systems. While current radionuclide/CT scanners obtain their respective images sequentially, MRI-compatible PET scanners have now been designed to allow data from both modalities to be obtained simultaneously without significant cross-interference of image quality [133]. Recently, Siemens Medical Solutions announced the development of a whole-body MR/PET system (Biograph™ mMR) for human patients.

Future strategies for cell labelling and imaging

In addition to MRI and radionuclide techniques, echocardiography may also be an option for cellular imaging in the future, probably through contrast enhancement by microbubble targeting. An example of this principle was provided in a recent rodent experiment, in which EPCs were transfected to express a cell surface marker protein (H-2Kk) that could be detected on ultrasonography by using microbubbles coated with a specific monoclonal antibody [134]. Another interesting possibility that has been evaluated to track transplanted pancreatic islet cells in vivo, but may have a broader application, is cell microencapsulation using semi-permeable capsules (e.g. alginate) that are embedded with contrast agents [e.g. bismuth sulphate, perfluorocarbon (PFCs)-hydrocarbons] [135, 136]. These contrasts may serve a dual function in that they seem to improve cell viability and function, while also rendering cells visible to various imaging modalities, including X-ray fluoroscopy, CT, ultrasound and ^{19}F-MRI. In the future, it is likely that more novel imaging strategies will be added to the armamentarium for the monitoring of cell therapies.

Integrated imaging of cell therapy in clinical studies

As depicted in Fig. 3, there is extensive scope for imaging to facilitate virtually every stage of the cell therapy process in patients with cardiovascular disease, from patient selection through to cell delivery, assessment of cell fate and follow-up of therapeutic outcome. One of the fundamental roles for imaging in clinical studies is to help characterise which patient and disease cohorts are most likely to respond to specific treatment strategies [137]. This requires rigorous baseline and follow-up evaluation of cardiac parameters that are relevant to disease context and are appropriate predictors of clinical outcome. Thus far, the benefit from autologous BM cell therapy after MI appears to be largely restricted to patients with the most severely impaired systolic function, as measured by LV ejection fraction [12]. It is therefore highly desirable for investigators to have access to objective, operator-independent modalities that can provide accurate and reproducible quantification of global ejection fraction, especially in the presence of LV dilatation and dysfunction [138]. To this end, a large number of clinical trials have favoured the use of MRI [70], as well as radionuclide angiography (gated blood pool scan), SPECT and PET over standard echocardiography or LV cineangiography. In the setting of established ischaemic cardiomyopathy, well-established PET or MRI techniques can also be used to distinguish hibernating myocardium from non-viable, post-infarct scar in order to shed light on the underlying cause of ischaemic dysfunction. This in turn may influence the choice of cell type(s) to be administered (e.g. pro-angiogenic BM or blood-derived cells for hibernation), as well as providing useful insight into the realistic likelihood of a therapeutic response.

With respect to follow-up after cell administration, different modalities can be combined to provide complementary information in the same subject to monitor important surrogate endpoints, including global LV volumes and ejection fraction, infarct size and thickness, myocardial perfusion, viability and metabolism. Such measures should be evaluated and quantified with the most accurate imaging techniques available using standardised protocols for data acquisition and analysis, by experts in the field [139]. However, rather than adopting a blanket approach to the assessment of surrogate parameters, the objective of imaging should remain focused on capturing the most meaningful endpoints with the most appropriate tools. Surveillance of regional contractile and diastolic function, infarct size and fibrosis burden may be especially prudent as these parameters can uncover early or subtle benefits from therapy before there is global improvement in cardiac performance [140, 141]. Other measurable indices may also emerge as having important implications for cell engraftment, such as microvascular obstruction, myocardial blood flow, haemorrhage, oedema, area at risk and oxygenation [142, 143].

Furthermore, one can also envisage the future utility of molecular imaging to assess specific pathophysiological substrates and unmask valuable information about the actions of cell transfer on key targets such as myocardial inflammation, cardiomyocyte apoptosis and angiogenesis [144]. Although not yet studied in the cell therapy setting, inflammation can be monitored after preclinical MI with optical tomography to detect fluorescent signal that is released when protease-activatable probes are recognised and cleaved by specific pro-inflammatory enzymes (e.g. matrix metalloproteinases, cathepsins) [145]. Cardiac cell apoptosis has also been assessed in human patients with acute MI [146], heart failure [147] and transplant rejection [148] through SPECT imaging of technetium-labelled annexin V, an endogenous protein which targets phosphatidylserine on apoptotic cell membranes. Preclinical feasibility has also been shown for MRI detection of annexin V conjugated to magnetofluorescent nanoparticles [149]. Similarly, myocardial angiogenesis can be monitored using several molecular imaging targets such as the $\alpha_v\beta_3$ integrin heterodimer or vascular endothelial growth factor (VEGF) receptors, which have been targeted with SPECT and PET probes in experimental and human MI [150–153].

The inclusion of noninvasive cell tracking in future clinical trials and mechanistic assessment of stem cell actions on the myocardium will provide direct insights not only into the mechanisms by which cell therapy strategies are successful, but also where they need to be optimised. Information about cell fate both in the short and long term will help to refocus efforts on refining the mechanics of cellular delivery and/or the functional biology of different stem cell candidates. Potentially, it will offer a means to identify likely non-responders (initial failure of cell delivery or rapid loss of cell engraftment), in whom repeat treatments may be warranted, or those patients who require close monitoring of non-cardiac toxicity (distribution of cells to other organs). For example, in the specific case of intramyocardial delivery, assessment of cell retention could convey immediate feedback regarding the success and precise location of injections. During longer follow-up, this information could then be used to help interpret regional changes in myocardial function, viability and perfusion.

At this stage, the path to human application requires further efforts to ensure that tracking techniques are closely tailored to answer specific scientific and clinical questions, while satisfying the strict standards of regulatory bodies, such as the FDA and European Medicines Agency. In all cases, the safety and efficiency of specific labelling and imaging techniques should be confirmed when applied to different cell types and disease settings. As a minimum, potential cytotoxicity needs careful assessment in terms of the viability, proliferative capacity, phenotype and intended function (e.g. angiogenesis, cardiomyocyte transdifferentiation) of the administered cells. Ideally, this evaluation should be extended over days to weeks after the initial incubation with the labelling agent, to exclude delayed adverse effects [102]. Considering that much of the proposed benefit of cell therapy appears to be mediated by paracrine mechanisms [154], future studies are also advised to investigate the effects of cell labelling on cytokine and growth factor synthesis.

For direct cell imaging, many of the labelling agents are already approved for human use, albeit for different purposes, and precedents exist for short-term radionuclide tracking of cell therapy in patients with IHD. Thus, at the present time, direct labelling appears more clinically feasible from the regulatory standpoint. Longer-term cell surveillance currently falls into the experimental realm of reporter gene labelling, which faces considerable challenges before clearance by regulatory bodies (e.g. Recombinant DNA Advisory Committee of the NIH and the FDA) will allow its application in humans. However, important early progress has been made by establishing the feasibility of indirect cell imaging in large animal studies, together with limited clinical experience [128]. Commercial interest and large-scale investment in the research, development and production of new labelling agents and imaging technologies will also play an important role in accelerating the transition of cell imaging to clinical practice.

Conclusion

The challenges created by the mechanistic uncertainties after cell transfer to the diseased heart have helped stimulate rapid progress in the fields of cell labelling and noninvasive tracking. Imaging has helped to elucidate several fundamental aspects of cell therapy, including the shortcomings of cell biology and current delivery methods as they relate to in vivo cell retention and engraftment. However, at present, no single labelling or imaging strategy fulfils all of the required need and further work is required to progress cell imaging effectively and safely to clinical trials and individual patient management. In tight conjunction with the indispensable roles that imaging already plays to assist cell delivery and patient follow-up, it is easy to envisage how a multimodal approach to cell tracking will provide great additive value to the future practice of cardiovascular cell therapy.

Acknowledgments

This work was supported by grant funding from NIH HL 88048 and the Mayo Foundation (MR-P). Dr. Psaltis is the recipient of an Overseas Biomedical Fellowship from the National Health and Medical Research Council of Australia and the Marjorie Hooper Overseas Fellowship from the Royal Australasian College of Physicians.

References

1. Gersh BJ, Simari RD, Behfar A, Terzic CM, Terzic A. Cardiac cell repair therapy: a clinical perspective. Mayo Clin Proc. 2009; 84:876–892. [PubMed: 19797777]
2. Strauer BE, Brehm M, Zeus T, Köstering M, Hernandez A, Sorg RV, et al. Repair of infarcted myocardium by autologous intracoronary mononuclear bone marrow cell transplantation in humans. Circulation. 2002; 106:1913–1918. [PubMed: 12370212]
3. Assmus B, Schächinger V, Teupe C, Britten M, Lehmann R, Döbert N, et al. Transplantation of progenitor cells and regeneration enhancement in acute myocardial infarction (TOP-CARE-AMI). Circulation. 2002; 106:3009–3017. [PubMed: 12473544]
4. Wollert KC, Meyer GP, Lotz J, Ringes-Lichtenberg S, Lippolt P, Breidenbach C, et al. Intracoronary autologous bone-marrow cell transfer after myocardial infarction: the BOOST randomised controlled clinical trial. Lancet. 2004; 364:141–148. [PubMed: 15246726]
5. Assmus B, Honold J, Schächinger V, Britten MB, Fischer-Rasokat U, Lehmann R, et al. Transcoronary transplantation of progenitor cells after myocardial infarction. N Engl J Med. 2006; 355:1222–1232. [PubMed: 16990385]
6. Lunde K, Solheim S, Aakhus S, Arnesen H, Abdelnoor M, Egeland T, et al. Intracoronary injection of mononuclear bone marrow cells in acute myocardial infarction. N Engl J Med. 2006; 355:1199–1209. [PubMed: 16990383]
7. Janssens S, Dubois C, Bogaert J, Theunissen K, Deroose C, Desmet W, et al. Autologous bone marrow-derived stem-cell transfer in patients with ST-segment elevation myocardial infarction: double-blind, randomised controlled trial. Lancet. 2006; 367:113–121. [PubMed: 16413875]
8. Fischer-Rasokat U, Assmus B, Seeger FH, Honold J, Leistner D, Fichtlscherer S, et al. A pilot trial to assess potential effects of selective intracoronary bone marrow-derived progenitor cell infusion in patients with nonischemic dilated cardiomyopathy: final 1-year results of the transplantation of progenitor cells and functional regeneration enhancement pilot trial in patients with nonischemic dilated cardiomyopathy. Circ Heart Fail. 2009; 2:417–423. [PubMed: 19808371]
9. Menasché P, Alfieri O, Janssens S, McKenna W, Reichenspurner H, Trinquart L, et al. The Myoblast Autologous Grafting in Ischemic Cardiomyopathy (MAGIC) trial: first randomized placebo-controlled study of myoblast transplantation. Circulation. 2008; 117:1189–1200. [PubMed: 18285565]
10. Hare JM, Traverse JH, Henry TD, Dib N, Strumpf RK, Schulman SP, et al. A randomized, double-blind, placebo-controlled, dose-escalation study of intravenous adult human mesenchymal stem cells (prochymal) after acute myocardial infarction. J Am Coll Cardiol. 2009; 54:2277–2286. [PubMed: 19958962]
11. Losordo DW, Schatz RA, White CJ, Udelson JE, Veereshwarayya V, Durgin M, et al. Intramyocardial transplantation of autologous CD34+ stem cells for intractable angina: a phase I/IIa double-blind, randomized controlled trial. Circulation. 2007; 115:3165–3172. [PubMed: 17562958]
12. Lipinski MJ, Biondi-Zoccai GG, Abbate A, Khianey R, Sheiban I, Bartunek J, et al. Impact of intracoronary cell therapy on left ventricular function in the setting of acute myocardial infarction: a collaborative systematic review and meta-analysis of controlled clinical trials. J Am Coll Cardiol. 2007; 50:1761–1767. [PubMed: 17964040]
13. Abdel-Latif A, Bolli R, Tleyjeh IM, Montori VM, Perin EC, Hornung CA, et al. Adult bone marrow-derived cells for cardiac repair: a systematic review and meta-analysis. Arch Intern Med. 2007; 167:989–997. [PubMed: 17533201]
14. Schächinger V, Erbs S, Elsässer A, Haberbosch W, Hambrecht R, Holschermann H, et al. Intracoronary bone marrow-derived progenitor cells in acute myocardial infarction. N Engl J Med. 2006; 355:1210–1221. [PubMed: 16990384]

15. Meyer GP, Wollert KC, Lotz J, Steffens J, Lippolt P, Fichtner S, et al. Intracoronary bone marrow cell transfer after myocardial infarction: eighteen months' follow-up data from the randomized, controlled BOOST (BOne marrOw transfer to enhance ST-elevation infarct regeneration) trial. Circulation. 2006; 113:1287–1294. [PubMed: 16520413]
16. Seeger FH, Tonn T, Krzossok N, Zeiher AM, Dimmeler S. Cell isolation procedures matter: a comparison of different isolation protocols of bone marrow mononuclear cells used for cell therapy in patients with acute myocardial infarction. Eur Heart J. 2007; 28:766–772. [PubMed: 17298974]
17. Brunskill SJ, Hyde CJ, Doree CJ, Watt SM, Martin-Rendon E. Route of delivery and baseline left ventricular ejection fraction, key factors of bone-marrow-derived cell therapy for ischaemic heart disease. Eur J Heart Fail. 2009; 11:887–896. [PubMed: 19654139]
18. Hou D, Youssef EA, Brinton TJ, Zhang P, Rogers P, Price ET, et al. Radiolabeled cell distribution after intramyocardial, intracoronary, and interstitial retrograde coronary venous delivery: implications for current clinical trials. Circulation. 2005; 112:I150–I156. [PubMed: 16159808]
19. Hofmann M, Wollert KC, Meyer GP, Menke A, Arseniev L, Hertenstein B, et al. Monitoring of bone marrow cell homing into the infarcted human myocardium. Circulation. 2005; 111:2198–2202. [PubMed: 15851598]
20. Erbs S, Linke A, Adams V, Lenk K, Thiele H, Diederich KW, et al. Transplantation of blood-derived progenitor cells after recanalization of chronic coronary artery occlusion: first randomized and placebo-controlled study. Circ Res. 2005; 97:756–762. [PubMed: 16151021]
21. Vulliet PR, Greeley M, Halloran SM, MacDonald KA, Kittleson MD. Intra-coronary arterial injection of mesenchymal stromal cells and microinfarction in dogs. Lancet. 2004; 363:783–784. [PubMed: 15016490]
22. Freyman T, Polin G, Osman H, Crary J, Lu M, Cheng L, et al. A quantitative, randomized study evaluating three methods of mesenchymal stem cell delivery following myocardial infarction. Eur Heart J. 2006; 27:1114–1122. [PubMed: 16510464]
23. Ly HQ, Hoshino K, Pomerantseva I, Kawase Y, Yoneyama R, Takewa Y, et al. In vivo myocardial distribution of multipotent progenitor cells following intracoronary delivery in a swine model of myocardial infarction. Eur Heart J. 2009; 30:2861–2868. [PubMed: 19687154]
24. Grossman PM, Han Z, Palasis M, Barry JJ, Lederman RJ. Incomplete retention after direct myocardial injection. Catheter Cardiovasc Interv. 2002; 55:392–397. [PubMed: 11870950]
25. Perin EC, Silva GV, Assad JA, Vela D, Buja LM, Sousa AL, et al. Comparison of intracoronary and transendocardial delivery of allogeneic mesenchymal cells in a canine model of acute myocardial infarction. J Mol Cell Cardiol. 2008; 44:486–495. [PubMed: 18061611]
26. Mitchell AJ, Sabondjian E, Sykes J, Deans L, Zhu W, Lu X, et al. Comparison of initial cell retention and clearance kinetics after subendocardial or subepicardial injections of endothelial progenitor cells in a canine myocardial infarction model. J Nucl Med. 2010; 51:413–417. [PubMed: 20150266]
27. Poh KK, Sperry E, Young RG, Freyman T, Barringhaus KG, Thompson CA. Repeated direct endomyocardial transplantation of allogeneic mesenchymal stem cells: safety of a high dose, "off-the-shelf", cellular cardiomyoplasty strategy. Int J Cardiol. 2007; 117:360–364. [PubMed: 16889857]
28. Psaltis PJ, Zannettino AC, Gronthos S, Worthley SG. Intramyocardial navigation and mapping for stem cell delivery. J Cardiovasc Transl Res. 2010; 3:135–146. [PubMed: 20560027]
29. Ince H, Petzsch M, Rehders TC, Chatterjee T, Nienaber CA. Transcatheter transplantation of autologous skeletal myoblasts in postinfarction patients with severe left ventricular dysfunction. J Endovasc Ther. 2004; 11:695–704. [PubMed: 15615560]
30. Smits PC, Nienaber C, Colombo A, Ince H, Carlino M, Theuns DA, et al. Myocardial repair by percutaneous cell transplantation of autologous skeletal myoblast as a stand alone procedure in post myocardial infarction chronic heart failure patients. Eurointervention. 2006; 1:417–424. [PubMed: 19755216]
31. de la Fuente LM, Stertzer SH, Argentieri J, Peñaloza E, Miano J, Koziner B, et al. Transendocardial autologous bone marrow in chronic myocardial infarction using a helical needle

catheter: 1-year follow-up in an open-label, nonrandomized, single-center pilot study (the TABMMI study). Am Heart J. 2007; 154:79. e1–79. e7. [PubMed: 17584556]

32. Duckers HJ, Houtgraaf J, Hehrlein C, Schofer J, Waltenberger J, Gershlick A, et al. Final results of a phase IIa, randomised, open-label trial to evaluate the percutaneous intramyocardial transplantation of autologous skeletal myoblasts in congestive heart failure patients: the SEISMIC trial. Eurointervention. 2011; 6:805–812. [PubMed: 21252013]
33. Psaltis PJ, Worthley SG. Endoventricular electromechanical mapping-the diagnostic and therapeutic utility of the NOGA® XP Cardiac Navigation System. J Cardiovasc Transl Res. 2009; 2:48–62. [PubMed: 20559969]
34. Kornowski R, Hong MK, Gepstein L, Goldstein S, Ellahham S, Ben-Haim SA, et al. Preliminary animal and clinical experiences using an electromechanical endocardial mapping procedure to distinguish infarcted from healthy myocardium. Circulation. 1998; 98:1116–1124. [PubMed: 9736599]
35. Fuchs S, Kornowski R, Shiran A, Pierre A, Ellahham S, Leon MB. Electromechanical characterization of myocardial hibernation in a pig model. Coron Artery Dis. 1999; 10:195–198. [PubMed: 10352897]
36. Botker HE, Lassen JF, Hermansen F, Wiggers H, Søgaard P, Kim WY, et al. Electromechanical mapping for detection of myocardial viability in patients with ischemic cardiomyopathy. Circulation. 2001; 103:1631–1637. [PubMed: 11273989]
37. Psaltis PJ, Carbone A, Leong DP, Lau DH, Nelson AJ, Kuchel T, et al. Assessment of myocardial fibrosis by endoventricular electromechanical mapping in experimental nonischemic cardiomyopathy. Int J Cardiovasc Imaging. 2011; 27:25–37. [PubMed: 20585861]
38. Perin EC, Dohmann HF, Borojevic R, Silva SA, Sousa AL, Mesquita CT, et al. Transendocardial, autologous bone marrow cell transplantation for severe, chronic ischemic heart failure. Circulation. 2003; 107:2294–2302. [PubMed: 12707230]
39. Krause K, Jaquet K, Schneider C, Haupt S, Lioznov MV, Otte KM, et al. Percutaneous intramyocardial stem cell injection in patients with acute myocardial infarction: first-in-man study. Heart. 2009; 95:1145–1152. [PubMed: 19336430]
40. Psaltis PJ, Carbone A, Nelson AJ, Lau DH, Jantzen T, Manavis J, et al. Reparative effects of allogeneic mesenchymal precursor cells delivered transendocardially in experimental nonischemic cardiomyopathy. JACC Cardiovasc Interv. 2010; 3:974–983. [PubMed: 20850099]
41. Chen SL, Fang WW, Ye F, Liu YH, Qian J, Shan SJ, et al. Effect on left ventricular function of intracoronary transplantation of autologous bone marrow mesenchymal stem cell in patients with acute myocardial infarction. Am J Cardiol. 2004; 94:92–95. [PubMed: 15219514]
42. Dib N, Menasche P, Bartunek JJ, Zeiher AM, Terzic A, Chronos NA, et al. Recommendations for successful training on methods of delivery of biologics for cardiac regeneration: a report of the International Society for Cardiovascular Translational Research. JACC Cardiovasc Interv. 2010; 3:265–275. [PubMed: 20298983]
43. Fernandes MR, Silva GV, Zheng Y, Oliveira EM, Cardoso CO, Canales J, et al. Validation of QwikStar Catheter for left ventricular electromechanical mapping with NOGA XP system. Tex Heart Inst J. 2008; 35:240–244. [PubMed: 18941605]
44. Perin EC, Silva GV, Fernandes MR, Munger T, Pandey A, Sehra R, et al. First experience with remote left ventricular mapping and transendocardial cell injection with a novel integrated magnetic navigation-guided electromechanical mapping system. Eurointervention. 2007; 3:142–148. [PubMed: 19737699]
45. Wei H, Ooi TH, Tan G, Lim SY, Qian L, Wong P, et al. Cell delivery and tracking in post-myocardial infarction cardiac stem cell therapy: an introduction for clinical researchers. Heart Fail Rev. 2010; 15:1–14. [PubMed: 19238541]
46. Dick AJ, Guttman MA, Raman VK, Peters DC, Pessanha BS, Hill JM, et al. Magnetic resonance fluoroscopy allows targeted delivery of mesenchymal stem cells to infarct borders in swine. Circulation. 2003; 108:2899–2904. [PubMed: 14656911]
47. Corti R, Badimon J, Mizsei G, Macaluso F, Lee M, Licato P, et al. Real time magnetic resonance guided endomyocardial local delivery. Heart. 2005; 91:348–353. [PubMed: 15710717]

48. Baklanov DV, de Muinck ED, Simons M, Moodie KL, Arbuckle BE, Thompson CA, et al. Live 3D echo guidance of catheter-based endomyocardial injection. Catheter Cardiovasc Interv. 2005; 65:340–345. [PubMed: 15832326]
49. Cheng Y, Sherman W, Yi G, Conditt G, Sheehy A, Martens T, et al. Real time 3D echo guided intramyocardial delivery of mesenchymal precursor cells in a chronic myocardial infarct ovine model using a novel catheter. J Am Coll Cardiol. 2009; 53:A41.
50. Saeed M, Saloner D, Weber O, Martin A, Henk C, Higgins C. MRI in guiding and assessing intramyocardial therapy. Eur Radiol. 2005; 15:851–863. [PubMed: 15856250]
51. Horvath KA, Mazilu D, Kocaturk O, Li M. Transapical aortic valve replacement under real-time magnetic resonance imaging guidance: experimental results with balloon-expandable and self-expanding stents. Eur J Cardiothorac Surg. 2011; 39:822–828. [PubMed: 20971017]
52. Fahrig R, Butts K, Wen Z, Saunders R, Kee ST, Sze DY, et al. Truly hybrid interventional MR/X-ray system: investigation of in vivo applications. Acad Radiol. 2001; 8:1200–1207. [PubMed: 11770916]
53. Vogl TJ, Balzer JO, Mack MG, Bett G, Oppelt A. Hybrid MR interventional imaging system: combined MR and angiography suites with single interactive table. Feasibility study in vascular liver tumor procedures. Eur Radiol. 2002; 12:1394–1400. [PubMed: 12042944]
54. Liu CY, Farahani K, Lu DS, Duckwiler G, Oppelt A. Safety of MRI-guided endovascular guidewire applications. J Magn Reson Imaging. 2000; 12:75–78. [PubMed: 10931566]
55. Lederman RJ, Guttman MA, Peters DC, Thompson RB, Sorger JM, Dick AJ, et al. Catheter-based endomyocardial injection with real-time magnetic resonance imaging. Circulation. 2002; 105:1282–1284. [PubMed: 11901036]
56. Karmarkar PV, Kraitchman DL, Izbudak I, Hofmann LV, Amado LC, Fritzges D, et al. MR-trackable intramyocardial injection catheter. Magn Reson Med. 2004; 51:1163–1172. [PubMed: 15170836]
57. de Silva R, Gutiérrez LF, Raval AN, McVeigh ER, Ozturk C, Lederman RJ. X-ray fused with magnetic resonance imaging (XFM) to target endomyocardial injections: validation in a swine model of myocardial infarction. Circulation. 2006; 114:2342–2350. [PubMed: 17101858]
58. Williams AR, Zambrano JP, Rodriguez J, Guerra D, Bonny G, McNiece I, et al. Merging three-dimensional cardiac MRI with electroanatomical mapping to guide transendocardial injections of mesenchymal stem cells. Circulation. 2010; 122:A15947.
59. Ladage D, Turnbull IC, Ishikawa K, Takewa Y, Rapti K, Morel C, et al. Delivery of gelfoam-enabled cells and vectors into the pericardial space using a percutaneous approach in a porcine model. Gene Ther. 2011 Published online April 21.
60. Azene NM, Ehtiati T, Fu Y, Flammang A, Guehring J, Gilson WD, et al. Intrapericardial delivery of visible microcapsules containing stem cells using xfm (x-ray fused with magnetic resonance imaging). J Cardiovasc Magn Reson. 2011; 13(Suppl 1):P26.
61. Hill JM, Dick AJ, Raman VK, Thompson RB, Yu ZX, Hinds KA, et al. Serial cardiac magnetic resonance imaging of injected mesenchymal stem cells. Circulation. 2003; 108:1009–1014. [PubMed: 12912822]
62. Stuckey DJ, Carr CA, Martin-Rendon E, Tyler DJ, Willmott C, Cassidy PJ, et al. Iron particles for noninvasive monitoring of bone marrow stromal cell engraftment into, and isolation of viable engrafted donor cells from, the heart. Stem Cells. 2006; 24:1968–1975. [PubMed: 16627684]
63. Chin BB, Nakamoto Y, Bulte JW, Pittenger MF, Wahl R, Kraitchman DL. 111In oxine labelled mesenchymal stem cell SPECT after intravenous administration in myocardial infarction. Nucl Med Commun. 2003; 24:1149–1154. [PubMed: 14569169]
64. Silva SA, Sousa AL, Haddad AF, Azevedo JC, Soares VE, Peixoto CM, et al. Autologous bone-marrow mononuclear cell transplantation after acute myocardial infarction: comparison of two delivery techniques. Cell Transplant. 2009; 18:343–352. [PubMed: 19558782]
65. Penicka M, Lang O, Widimsky P, Kobylka P, Kozak T, Vanek T, et al. One-day kinetics of myocardial engraftment after intracoronary injection of bone marrow mononuclear cells in patients with acute and chronic myocardial infarction. Heart. 2007; 93:837–841. [PubMed: 17309910]
66. Goussetis E, Manginas A, Koutelou M, Peristeri I, Theodosaki M, Kollaros N, et al. Intracoronary infusion of CD133+ and CD133-CD34+ selected autologous bone marrow progenitor cells in

patients with chronic ischemic cardiomyopathy: cell isolation, adherence to the infarcted area, and body distribution. Stem Cells. 2006; 24:2279–2283. [PubMed: 16794269]

67. Kang WJ, Kang HJ, Kim HS, Chung JK, Lee MC, Lee DS. Tissue distribution of 18F-FDG-labeled peripheral hematopoietic stem cells after intracoronary administration in patients with myocardial infarction. J Nucl Med. 2006; 47:1295–1301. [PubMed: 16883008]
68. Doyle B, Kemp BJ, Chareonthaitawee P, Reed C, Schmeckpeper J, Sorajja P, et al. Dynamic tracking during intracoronary injection of 18F-FDG-labeled progenitor cell therapy for acute myocardial infarction. J Nucl Med. 2007; 48:1708–1714. [PubMed: 17909258]
69. de Waha S, Fuernau G, Eitel I, Lurz P, Desch S, Schuler G, et al. Measuring treatment effects in clinical trials using cardiac MRI. Curr Cardiovasc Imaging Rep. 2011 Published online January 19.
70. Ye Y, Bogaert J. Cell therapy in myocardial infarction: emphasis on the role of MRI. Eur Radiol. 2008; 18:548–569. [PubMed: 17922278]
71. Wunderbaldinger P, Josephson L, Weissleder R. Crosslinked iron oxides (CLIO): a new platform for the development of targeted MR contrast agents. Acad Radiol. 2002; 9(Suppl 2):S304–S306. [PubMed: 12188255]
72. Park KS, Tae J, Choi B, Kim YS, Moon C, Kim SH, et al. Characterization, in vitro cytotoxicity assessment, and in vivo visualization of multimodal, RITC-labeled, silica-coated magnetic nanoparticles for labeling human cord blood-derived mesenchymal stem cells. Nanomedicine. 2010; 6:263–276. [PubMed: 19699324]
73. Himes N, Min JY, Lee R, Brown C, Shea J, Huang X, et al. In vivo MRI of embryonic stem cells in a mouse model of myocardial infarction. Magn Reson Med. 2004; 52:1214–1219. [PubMed: 15508153]
74. Küstermann E, Roell W, Breitbach M, Wecker S, Wiedermann D, Buehrle C, et al. Stem cell implantation in ischemic mouse heart: a high-resolution magnetic resonance imaging investigation. NMR Biomed. 2005; 18:362–370. [PubMed: 15948224]
75. Amsalem Y, Mardor Y, Feinberg MS, Landa N, Miller L, Daniels D, et al. Iron-oxide labeling and outcome of transplanted mesenchymal stem cells in the infarcted myocardium. Circulation. 2007; 116:I38–I45. [PubMed: 17846324]
76. Kraitchman DL, Heldman AW, Atalar E, Amado LC, Martin BJ, Pittenger MF, et al. In vivo magnetic resonance imaging of mesenchymal stem cells in myocardial infarction. Circulation. 2003; 107:2290–2293. [PubMed: 12732608]
77. Bulte JW, Kostura L, Mackay A, Karmarkar PV, Izbudak I, Atalar E, et al. Feridex-labeled mesenchymal stem cells: cellular differentiation and MR assessment in a canine myocardial infarction model. Acad Radiol. 2005; 12(Suppl 1):S2–S6. [PubMed: 16106536]
78. Terrovitis JV, Bulte JW, Sarvananthan S, Crowe LA, Sarathchandra P, Batten P, et al. Magnetic resonance imaging of ferumoxide-labeled mesenchymal stem cells seeded on collagen scaffolds-relevance to tissue engineering. Tissue Eng. 2006; 12:2765–2775. [PubMed: 17518646]
79. Stuckey DJ, Ishii H, Chen QZ, Boccaccini AR, Hansen U, Carr CA, et al. Magnetic resonance imaging evaluation of remodeling by cardiac elastomeric tissue scaffold biomaterials in a rat model of myocardial infarction. Tissue Eng Part A. 2010; 16:3395–3402. [PubMed: 20528670]
80. Kanematsu M, Kondo H, Goshima S, Kato H, Tsuge U, Hirose Y, et al. Imaging liver metastases: review and update. Eur J Radiol. 2006; 58:217–228. [PubMed: 16406434]
81. Wu L, Cao Y, Liao C, Huang J, Gao F. Diagnostic performance of USPIO-enhanced MRI for lymph-node metastases in different body regions: a meta-analysis. Eur J Radiol. 2010 Published online January 2.
82. de Vries IJ, Lesterhuis WJ, Barentsz JO, Verdijk P, van Krieken JH, Boerman OC, et al. Magnetic resonance tracking of dendritic cells in melanoma patients for monitoring of cellular therapy. Nat Biotechnol. 2005; 23:1407–1413. [PubMed: 16258544]
83. Zhu J, Zhou L, XingWu F. Tracking neural stem cells in patients with brain trauma. N Engl J Med. 2006; 355:2376–2378. [PubMed: 17135597]
84. Chen IY, Greve JM, Gheysens O, Willmann JK, Rodriguez-Porcel M, Chu P, et al. Comparison of optical bioluminescence reporter gene and superparamagnetic iron oxide MR contrast agent as cell

markers for noninvasive imaging of cardiac cell transplantation. Mol Imaging Biol. 2009; 11:178–187. [PubMed: 19034584]

85. Arbab AS, Yocum GT, Rad AM, Khakoo AY, Fellowes V, Read EJ, et al. Labeling of cells with ferumoxides-protamine sulfate complexes does not inhibit function or differentiation capacity of hematopoietic or mesenchymal stem cells. NMR Biomed. 2005; 18:553–559. [PubMed: 16229060]
86. Suzuki Y, Zhang S, Kundu P, Yeung AC, Robbins RC, Yang PC. In vitro comparison of the biological effects of three transfection methods for magnetically labeling mouse embryonic stem cells with ferumoxides. Magn Reson Med. 2007; 57:1173–1179. [PubMed: 17534917]
87. Yang JX, Tang WL, Wang XX. Superparamagnetic iron oxide nanoparticles may affect endothelial progenitor cell migration ability and adhesion capacity. Cytotherapy. 2010; 12:251–259. [PubMed: 20196696]
88. Schäfer R, Kehlbach R, Müller M, Bantleon R, Kluba T, Ayturan M, et al. Labeling of human mesenchymal stromal cells with superparamagnetic iron oxide leads to a decrease in migration capacity and colony formation ability. Cytotherapy. 2009; 11:68–78. [PubMed: 19191056]
89. Kostura L, Kraitchman DL, Mackay AM, Pittenger MF, Bulte JW. Feridex labeling of mesenchymal stem cells inhibits chondrogenesis but not adipogenesis or osteogenesis. NMR Biomed. 2004; 17:513–517. [PubMed: 15526348]
90. Bos C, Delmas Y, Desmoulière A, Solanilla A, Hauger O, Grosset C, et al. In vivo MR imaging of intravascularly injected magnetically labeled mesenchymal stem cells in rat kidney and liver. Radiology. 2004; 233:781–789. [PubMed: 15486216]
91. Terrovitis J, Stuber M, Youssef A, Preece S, Leppo M, Kizana E, et al. Magnetic resonance imaging overestimates ferumoxide-labeled stem cell survival after transplantation in the heart. Circulation. 2008; 117:1555–11562. [PubMed: 18332264]
92. van den Bos EJ, Baks T, Moelker AD, Kerver W, van Geuns RJ, van der Giessen WJ, et al. Magnetic resonance imaging of haemorrhage within reperfused myocardial infarcts: possible interference with iron oxide-labelled cell tracking? Eur Heart J. 2006; 27:1620–1626. [PubMed: 16751204]
93. Mani V, Adler E, Briley-Saebo KC, Bystrup A, Fuster V, Keller G, et al. Serial in vivo positive contrast MRI of iron oxide-labeled embryonic stem cell-derived cardiac precursor cells in a mouse model of myocardial infarction. Magn Reson Med. 2008; 60:73–81. [PubMed: 18581415]
94. Zhou R, Idiyatullin D, Moeller S, Corum C, Zhang H, Qiao H, et al. SWIFT detection of SPIO-labeled stem cells grafted in the myocardium. Magn Reson Med. 2010; 63:1154–1161. [PubMed: 20432286]
95. Tran LA, Krishnamurthy R, Muthupillai R, Cabreira-Hansen Mda G, Willerson JT, Perin EC, et al. Gadonanotubes as magnetic nanolabels for stem cell detection. Biomaterials. 2010; 31:9482–9491. [PubMed: 20965562]
96. Adler ED, Bystrup A, Briley-Saebo KC, Mani V, Young W, Giovanonne S, et al. In vivo detection of embryonic stem cell-derived cardiovascular progenitor cells using Cy3-labeled Gado-fluorine M in murine myocardium. JACC Cardiovasc Imaging. 2009; 2:1114–1122. [PubMed: 19761992]
97. Partlow KC, Chen J, Brant JA, Neubauer AM, Meyerrose TE, Creer MH, et al. 19F magnetic resonance imaging for stem/progenitor cell tracking with multiple unique perfluorocarbon nanobeacons. FASEB J. 2007; 21:1647–1654. [PubMed: 17284484]
98. Rodriguez-Porcel M, Brinton TJ, Chen IY, Gheysens O, Lyons J, Ikeno F, et al. Reporter gene imaging following percutaneous delivery in swine moving toward clinical applications. J Am Coll Cardiol. 2008; 51:595–597. [PubMed: 18237691]
99. Terrovitis J, Lautamäki R, Bonios M, Fox J, Engles JM, Yu J, et al. Noninvasive quantification and optimization of acute cell retention by in vivo positron emission tomography after intra-myocardial cardiac-derived stem cell delivery. J Am Coll Cardiol. 2009; 54:1619–1626. [PubMed: 19833262]
100. Brenner W, Aicher A, Eckey T, Massoudi S, Zuhayra M, Koehl U, et al. 111In-labeled CD34+ hematopoietic progenitor cells in a rat myocardial infarction model. J Nucl Med. 2004; 45:512–518. [PubMed: 15001696]

101. Nowak B, Weber C, Schober A, Zeiffer U, Liehn EA, von Hundelshausen P, et al. Indium-111 oxine labelling affects the cellular integrity of haematopoietic progenitor cells. Eur J Nucl Med Mol Imaging. 2007; 34:715–721. [PubMed: 17096094]
102. Gholamrezanezhad A, Mirpour S, Ardekani JM, Bagheri M, Alimoghadam K, Yarmand S, et al. Cytotoxicity of 111In-oxine on mesenchymal stem cells: a time-dependent adverse effect. Nucl Med Commun. 2009; 30:210–216. [PubMed: 19262283]
103. Yoon JK, Park BN, Shim WY, Shin JY, Lee G, Ahn YH. In vivo tracking of 111In-labeled bone marrow mesenchymal stem cells in acute brain trauma model. Nucl Med Biol. 2010; 37:381–388. [PubMed: 20346878]
104. Gildehaus FJ, Haasters F, Drosse I, Wagner E, Zach C, Mutschler W, et al. Impact of indium-111 oxine labelling on viability of human mesenchymal stem cells in vitro, and 3D cell-tracking using SPECT/CT in vivo. Mol Imaging Biol. 2010 Published online November 17.
105. Huang J, Lee CC, Sutcliffe JL, Cherry SR, Tarantal AF. Radiolabeling rhesus monkey CD34+ hematopoietic and mesenchymal stem cells with 64Cu-pyruvaldehyde-bis(N4-methyl-thiosemicarbazone) for microPET imaging. Mol Imaging. 2008; 7:1–11. [PubMed: 18384718]
106. Aicher A, Brenner W, Zuhayra M, Badorff C, Massoudi S, Assmus B, et al. Assessment of the tissue distribution of transplanted human endothelial progenitor cells by radioactive labeling. Circulation. 2003; 107:2134–2139. [PubMed: 12695305]
107. Lyngbaek S, Ripa RS, Haack-Sørensen M, Cortsen A, Kragh L, Andersen CB, et al. Serial in vivo imaging of the porcine heart after percutaneous, intramyocardially injected 111In-labeled human mesenchymal stromal cells. Int J Cardiovasc Imaging. 2010; 26:273–284. [PubMed: 19921546]
108. Dedobbeleer C, Blocklet D, Toungouz M, Lambermont M, Unger P, Degaute JP, et al. Myocardial homing and coronary endothelial function after autologous blood CD34+ progenitor cells intracoronary injection in the chronic phase of myocardial infarction. J Cardiovasc Pharmacol. 2009; 53:480–485. [PubMed: 19433985]
109. Schächinger V, Aicher A, Döbert N, Röver R, Diener J, Fichtlscherer S, et al. Pilot trial on determinants of progenitor cell recruitment to the infarcted human myocardium. Circulation. 2008; 118:1425–1432. [PubMed: 18794392]
110. Seeger FH, Zeiher AM, Dimmeler S. Cell-enhancement strategies for the treatment of ischemic heart disease. Nat Clin Pract Cardiovasc Med. 2007; 4(Suppl 1):S110–S113. [PubMed: 17230207]
111. Cao F, Lin S, Xie X, Ray P, Patel M, Zhang X, et al. In vivo visualization of embryonic stem cell survival, proliferation, and migration after cardiac delivery. Circulation. 2006; 113:1005–1014. [PubMed: 16476845]
112. Nelson TJ, Martinez-Fernandez A, Yamada S, Perez-Terzic C, Ikeda Y, Terzic A. Repair of acute myocardial infarction by human stemness factors induced pluripotent stem cells. Circulation. 2009; 120:408–416. [PubMed: 19620500]
113. Bhaumik S, Gambhir SS. Optical imaging of Renilla luciferase reporter gene expression in living mice. Proc Natl Acad Sci U S A. 2002; 99:377–382. [PubMed: 11752410]
114. Rodriguez-Porcel M, Gheysens O, Chen IY, Wu JC, Gambhir SS. Image-guided cardiac cell delivery using high-resolution small-animal ultrasound. Mol Ther. 2005; 12:1142–1147. [PubMed: 16111921]
115. Wu JC, Chen IY, Sundaresan G, Min JJ, De A, Qiao JH, et al. Molecular imaging of cardiac cell transplantation in living animals using optical bioluminescence and positron emission tomography. Circulation. 2003; 108:1302–1305. [PubMed: 12963637]
116. Terrovitis J, Kwok KF, Lautamäki R, Engles JM, Barth AS, Kizana E, et al. Ectopic expression of the sodium-iodide symporter enables imaging of transplanted cardiac stem cells in vivo by single-photon emission computed tomography or positron emission tomography. J Am Coll Cardiol. 2008; 52:1652–1660. [PubMed: 18992656]
117. Gilad AA, Winnard PT Jr, van Zijl PC, Bulte JW. Developing MR reporter genes: promises and pitfalls. NMR Biomed. 2007; 20:275–290. [PubMed: 17451181]
118. Naumova AV, Reinecke H, Yarnykh V, Deem J, Yuan C, Murry CE. Ferritin overexpression for noninvasive magnetic resonance imaging-based tracking of stem cells transplanted into the heart. Mol Imaging. 2010; 9:201–210. [PubMed: 20643023]

119. Massoud TF, Gambhir SS. Molecular imaging in living subjects: seeing fundamental biological processes in a new light. Genes Dev. 2003; 17:545–580. [PubMed: 12629038]
120. Rodriguez-Porcel M. In vivo imaging and monitoring of transplanted stem cells: clinical applications. Curr Cardiol Rep. 2010; 12:51–58. [PubMed: 20425184]
121. Terrovitis JV, Smith RR, Marbán E. Assessment and optimization of cell engraftment after transplantation into the heart. Circ Res. 2010; 106:479–494. [PubMed: 20167944]
122. Gyöngyösi M, Blanco J, Marian T, Trón L, Petneházy O, Petrasi Z, et al. Serial noninvasive in vivo positron emission tomographic tracking of percutaneously intramyocardially injected autologous porcine mesenchymal stem cells modified for transgene reporter gene expression. Circ Cardiovasc Imaging. 2008; 1:94–103. [PubMed: 19808526]
123. Kang JH, Lee DS, Paeng JC, Lee JS, Kim YH, Lee YJ, et al. Development of a sodium/iodide symporter (NIS)-transgenic mouse for imaging of cardiomyocyte-specific reporter gene expression. J Nucl Med. 2005; 46:479–483. [PubMed: 15750162]
124. MacLaren DC, Gambhir SS, Satyamurthy N, Barrio JR, Sharfstein S, Toyokuni T, et al. Repetitive, non-invasive imaging of the dopamine D2 receptor as a reporter gene in living animals. Gene Ther. 1999; 6:785–791. [PubMed: 10505102]
125. Cohen B, Dafni H, Meir G, Harmelin A, Neeman M. Ferritin as an endogenous MRI reporter for noninvasive imaging of gene expression in C6 glioma tumors. Neoplasia. 2005; 7:109–117. [PubMed: 15802016]
126. Bengel FM, Anton M, Richter T, Simoes MV, Haubner R, Henke J, et al. Noninvasive imaging of transgene expression by use of positron emission tomography in a pig model of myocardial gene transfer. Circulation. 2003; 108:2127–2133. [PubMed: 14530205]
127. Willmann JK, Paulmurugan R, Rodriguez-Porcel M, Stein W, Brinton TJ, Connolly AJ, et al. Imaging gene expression in human mesenchymal stem cells: from small to large animals. Radiology. 2009; 252:117–127. [PubMed: 19366903]
128. Yaghoubi SS, Jensen MC, Satyamurthy N, Budhiraja S, Paik D, Czernin J, et al. Noninvasive detection of therapeutic cytolytic T cells with 18F-FHBG PET in a patient with glioma. Nat Clin Pract Oncol. 2009; 6:53–58. [PubMed: 19015650]
129. Li Z, Suzuki Y, Huang M, Cao F, Xie X, Connolly AJ, et al. Comparison of reporter gene and iron particle labeling for tracking fate of human embryonic stem cells and differentiated endothelial cells in living subjects. Stem Cells. 2008; 26:864–873. [PubMed: 18218820]
130. Qiao H, Zhang H, Zheng Y, Ponde DE, Shen D, Gao F, et al. Embryonic stem cell grafting in normal and infarcted myocardium: serial assessment with MR imaging and PET dual detection. Radiology. 2009; 250:821–829. [PubMed: 19244049]
131. Shen D, Liu D, Cao Z, Acton PD, Zhou R. Coregistration of magnetic resonance and single photon emission computed tomography images for noninvasive localization of stem cells grafted in the infarcted rat myocardium. Mol Imaging Biol. 2007; 9:24–31. [PubMed: 17053860]
132. Wang J, Zhang S, Rabinovich B, Bidaut L, Soghomonyan S, Alauddin MM, et al. Human CD34+ cells in experimental myocardial infarction: long-term survival, sustained functional improvement, and mechanism of action. Circ Res. 2010; 106:1904–1911. [PubMed: 20448213]
133. Catana C, Procissi D, Wu Y, Judenhofer MS, Qi J, Pichler BJ, et al. Simultaneous in vivo positron emission tomography and magnetic resonance imaging. Proc Natl Acad Sci U S A. 2008; 105:3705–3710. [PubMed: 18319342]
134. Kuliszewski MA, Fujii H, Liao C, Smith AH, Xie A, Lindner JR, et al. Molecular imaging of endothelial progenitor cell engraftment using contrast-enhanced ultrasound and targeted microbubbles. Cardiovasc Res. 2009; 83:653–662. [PubMed: 19564152]
135. Barnett BP, Kraitchman DL, Lauzon C, Magee CA, Walczak P, Gilson WD, et al. Radiopaque alginate microcapsules for X-ray visualization and immunoprotection of cellular therapeutics. Mol Pharm. 2006; 3:531–538. [PubMed: 17009852]
136. Barnett BP, Ruiz-Cabello J, Hota P, Liddell R, Walczak P, Howland V, et al. Fluorocapsules for improved function, immunoprotection, and visualization of cellular therapeutics with MR, US, and CT imaging. Radiology. 2011; 258:182–191. [PubMed: 20971778]
137. Penn MS. Stem-cell therapy after acute myocardial infarction: the focus should be on those at risk. Lancet. 2006; 367:87–88. [PubMed: 16413856]

138. Bellenger NG, Burgess MI, Ray SG, Lahiri A, Coats AJ, Cleland JG, et al. Comparison of left ventricular ejection fraction and volumes in heart failure by echocardiography, radionuclide ventriculography and cardiovascular magnetic resonance, are they interchangeable? Eur Heart J. 2000; 21:1387–1396. [PubMed: 10952828]
139. Arnesen H, Lunde K, Aakhus S, Forfang K. Cell therapy in myocardial infarction. Lancet. 2007; 369:2142–2143. [PubMed: 17604783]
140. Schaefer A, Meyer GP, Fuchs M, Klein G, Kaplan M, Wollert KC, et al. Impact of intracoronary bone marrow cell transfer on diastolic function in patients after acute myocardial infarction: results from the BOOST trial. Eur Heart J. 2006; 27:929–935. [PubMed: 16510465]
141. Assmus B, Rolf A, Erbs S, Elsässer A, Haberbosch W, Hambrecht R, et al. Clinical outcome 2 years after intracoronary administration of bone marrow-derived progenitor cells in acute myocardial infarction. Circ Heart Fail. 2010; 3:89–96. [PubMed: 19996415]
142. Aletras AH, Tilak GS, Natanzon A, Hsu LY, Gonzalez FM, Hoyt RF Jr, et al. Retrospective determination of the area at risk for reperfused acute myocardial infarction with T2-weighted cardiac magnetic resonance imaging: histopathological and displacement encoding with stimulated echoes (DENSE) functional validations. Circulation. 2006; 113:1865–1870. [PubMed: 16606793]
143. McCommis KS, O'Connor R, Lesniak D, Lyons M, Woodard PK, Gropler RJ, et al. Quantification of global myocardial oxygenation in humans: initial experience. J Cardiovasc Magn Reson. 2010; 12:34. [PubMed: 20525217]
144. Nahrendorf M, Sosnovik DE, French BA, Swirski FK, Bengel F, Sadeghi MM, et al. Multimodality cardiovascular molecular imaging, part II. Circ Cardiovasc Imaging. 2009; 2:56–70. [PubMed: 19808565]
145. Nahrendorf M, Sosnovik DE, Waterman P, Swirski FK, Pande AN, Aikawa E, et al. Dual channel optical tomographic imaging of leukocyte recruitment and protease activity in the healing myocardial infarct. Circ Res. 2007; 100:1218–1225. [PubMed: 17379832]
146. Hofstra L, Liem IH, Dumont EA, Boersma HH, van Heerde WL, Doevendans PA, et al. Visualisation of cell death in vivo in patients with acute myocardial infarction. Lancet. 2000; 356:209–212. [PubMed: 10963199]
147. Kietselaer BL, Reutelingsperger CP, Boersma HH, Heidendal GA, Liem IH, Crijns HJ, et al. Noninvasive detection of programmed cell loss with 99mTc-labeled annexin A5 in heart failure. J Nucl Med. 2007; 48:562–567. [PubMed: 17401092]
148. Narula J, Acio ER, Narula N, Samuels LE, Fyfe B, Wood D, et al. Annexin-V imaging for noninvasive detection of cardiac allograft rejection. Nat Med. 2001; 7:1347–1352. [PubMed: 11726976]
149. Sosnovik DE, Schellenberger EA, Nahrendorf M, Novikov MS, Matsui T, Dai G, et al. Magnetic resonance imaging of cardiomyocyte apoptosis with a novel magneto-optical nanoparticle. Magn Reson Med. 2005; 54:718–724. [PubMed: 16086367]
150. Meoli DF, Sadeghi MM, Krassilnikova S, Bourke BN, Giordano FJ, Dione DP, et al. Noninvasive imaging of myocardial angiogenesis following experimental myocardial infarction. J Clin Invest. 2004; 113:1684–1691. [PubMed: 15199403]
151. Makowski MR, Ebersberger U, Nekolla S, Schwaiger M. In vivo molecular imaging of angiogenesis, targeting αvβ3 integrin expression, in a patient after acute myocardial infarction. Eur Heart J. 2008; 29:2201. [PubMed: 18375397]
152. Rodriguez-Porcel M, Cai W, Gheysens O, Willmann JK, Chen K, Wang H, et al. Imaging of VEGF receptor in a rat myocardial infarction model using PET. J Nucl Med. 2008; 49:667–673. [PubMed: 18375924]
153. Rodriguez-Porcel M. Non-invasive monitoring of angiogenesis in cardiology. Curr Cardiovasc Imaging Rep. 2009; 2:59–66. [PubMed: 20508836]
154. Psaltis PJ, Zannettino AC, Worthley SG, Gronthos S. Concise review: mesenchymal stromal cells: potential for cardiovascular repair. Stem Cells. 2008; 26:2201–2210. [PubMed: 18599808]
155. Gyöngyösi M, Lang I, Dettke M, Beran G, Graf S, Sochor H, et al. Combined delivery approach of bone marrow mononuclear stem cells early and late after myocardial infarction: the MYSTAR

prospective, randomized study. Nat Clin Pract Cardiovasc Med. 2009; 6:70–81. [PubMed: 19002124]

156. Briguori C, Reimers B, Sarais C, Napodano M, Pascotto P, Azzarello G, et al. Direct intramyocardial percutaneous delivery of autologous bone marrow in patients with refractory myocardial angina. Am Heart J. 2006; 151:674–680. [PubMed: 16504630]
157. Beeres SL, Bax JJ, Dibbets P, Stokkel MP, Zeppenfeld K, Fibbe WE, et al. Effect of intramyocardial injection of autologous bone marrow-derived mononuclear cells on perfusion, function, and viability in patients with drug-refractory chronic ischemia. J Nucl Med. 2006; 47:574–580. [PubMed: 16595489]
158. Fuchs S, Kornowski R, Weisz G, Satler LF, Smits PC, Okubagzi P, et al. Safety and feasibility of transendocardial autologous bone marrow cell transplantation in patients with advanced heart disease. Am J Cardiol. 2006; 97:823–829. [PubMed: 16516583]
159. Tse HF, Thambar S, Kwong YL, Rowlings P, Bellamy G, McCrohon J, et al. Prospective randomized trial of direct endomyocardial implantation of bone marrow cells for treatment of severe coronary artery diseases (PROTECT-CAD trial). Eur Heart J. 2007; 28:2998–3005. [PubMed: 17984132]
160. van Ramshorst J, Bax JJ, Beeres SL, Dibbets-Schneider P, Roes SD, Stokkel MP, et al. Intramyocardial bone marrow cell injection for chronic myocardial ischemia: a randomized controlled trial. JAMA. 2009; 301:1997–2004. [PubMed: 19454638]
161. Dib N, Dinsmore J, Lababidi Z, White B, Moravec S, Campbell A, et al. One-year follow-up of feasibility and safety of the first U.S., randomized, controlled study using 3-dimensional guided catheter-based delivery of autologous skeletal myoblasts for ischemic cardiomyopathy (CAuSMIC study). JACC Cardiovasc Interv. 2009; 2:9–16. [PubMed: 19463392]
162. Kraitchman DL, Bulte JW. Imaging of stem cells using MRI. Basic Res Cardiol. 2008; 103:105–113. [PubMed: 18324366]

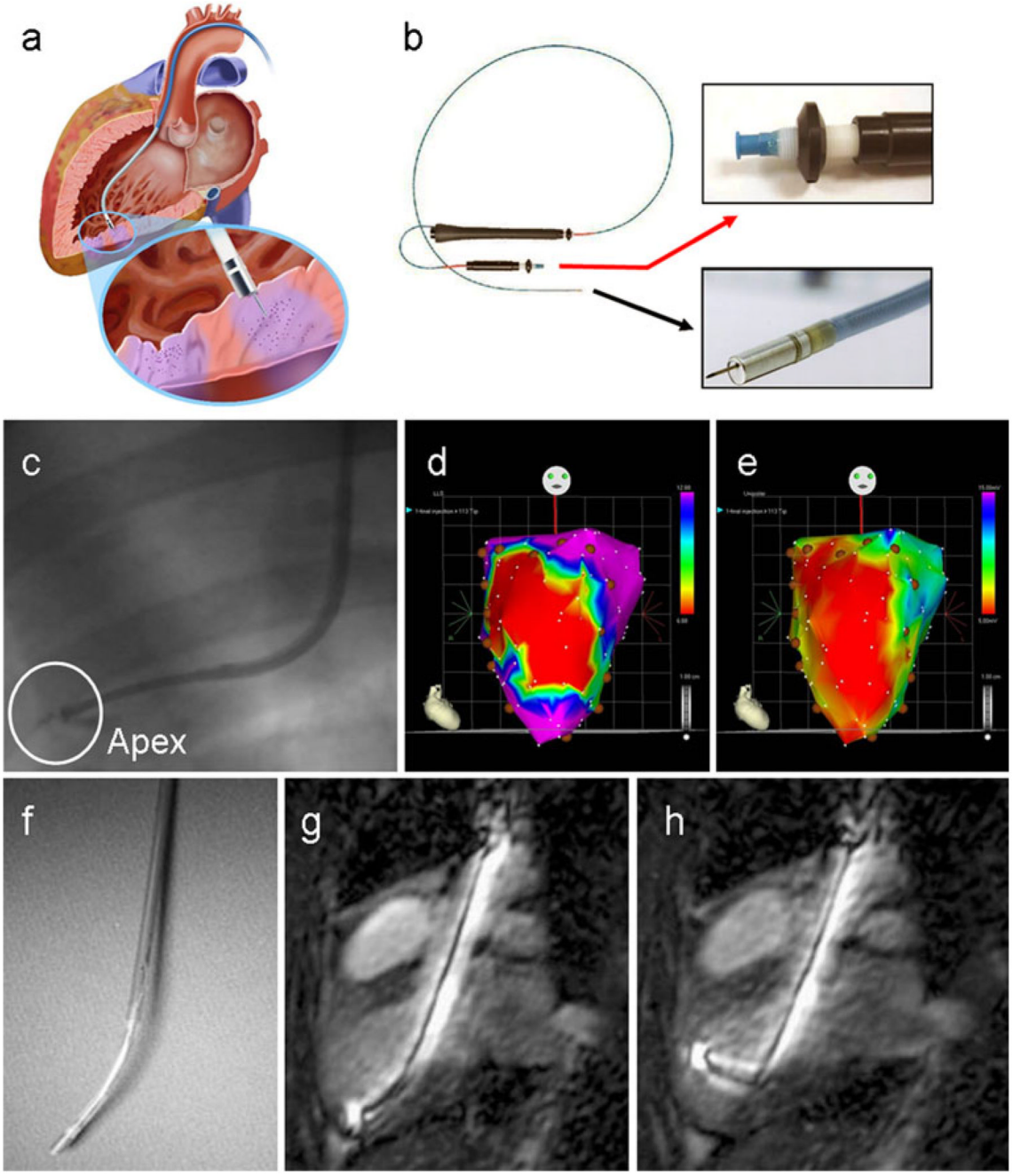

Fig. 1.

Imaging navigation of transendocardial delivery. **a** Schematic displays an injection catheter passed across the aortic valve into the left ventricular cavity, with its needle tip extruded into the endomyocardium of the inferoposterior wall (*inset*). *Purple areas* of myocardium highlight two injection sites (image kindly provided by Biologics Delivery Systems Group, Cordis Corporation). **b** MyoStar™ injection catheter. The *black arrow* points to an inset of the catheter tip with extended 27 gauge needle and the *red arrow* to the adjustable injector thumb knob and Luer-lock fitting for connection to the injection syringe. **c** Conventional X-ray fluoroscopic guidance of catheter positioning near the left ventricular apex (adapted with

permission from [98]). **d, e** Examples of electromechanical mapping images in a patient with anterior myocardial infarction, with linear local shortening (**d**) and unipolar voltage (**e**) maps shown in the anteroposterior projection. The *red areas* correspond to the infarct territory, with coupling of the reduced electrical signal and mechanical function over the anterior left ventricular wall. In this case, intramyocardial injections of cell therapy were administered in a peri-infarct distribution, as indicated by the *brown circular markers* (reproduced with permission from [33]). **f–h** MR guidance of catheter-based injection. The flexibility of the custom MR-compatible injection catheter (**f**) enables its manipulation to all regions of the endocardial surface. (**g, h**) Active catheters generate a high signal intensity for easy visualisation inside the ventricular cavity using real-time MR steady-state free precession imaging (reproduced with permission from [162])

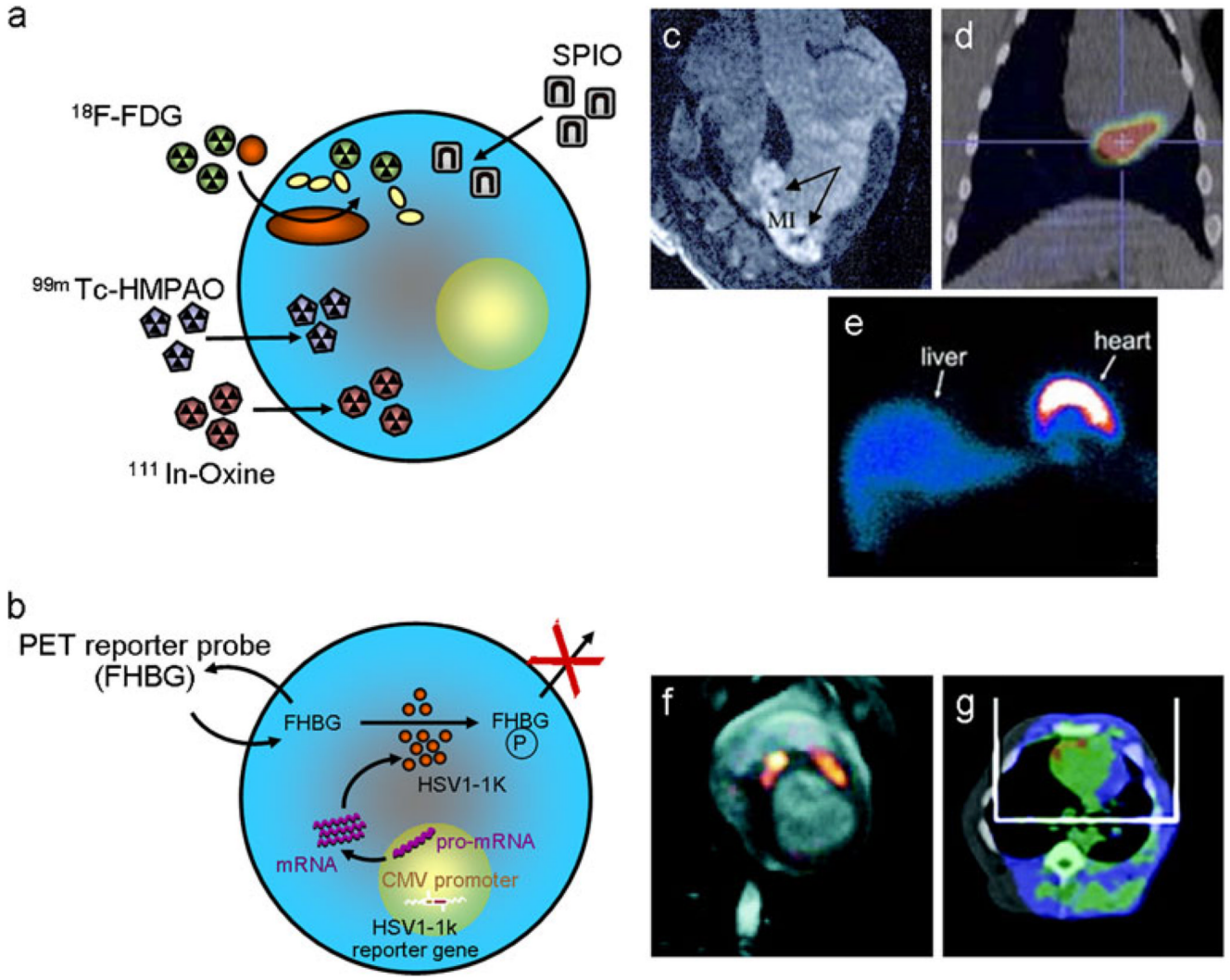

Fig. 2.

Direct and indirect labelling for cell detection. Schematic depictions of the strategies used for **a** direct labelling and **b** indirect reporter gene labelling of cells prior to their administration, with examples of their imaging using MRI, SPECT and PET. **c** Delayed enhancement MRI showing infarcted myocardium (hyperintense) containing hypointense lesions from iron-labelled MSCs (*arrows*) which were injected 24 h earlier (adapted with permission from [76]). **d** Combined PET/CT image showing in vivo detection of ^{18}F-fluorodeoxyglucose (FDG)-labelled progenitor cells within the inferolateral territory of the left ventricle after intracoronary delivery (borrowed with permission from [68]). **e** SPECT-based imaging of the biodistribution of ^{99m}Tc-hexamethylpropylenamineoxine (HMPAO)-labelled BM progenitor cells 1 h after delivery to a patient with chronic ischaemic cardiomyopathy. Anterior view of chest and upper abdomen is shown with *black* indicating no uptake and *blue-red-yellow-white* showing the gradient of increasing signal (reproduced with permission from [66]). **f** Fusion image of MRI (grey scale) and ^{18}F-FHBG PET (hot scale) showing accumulation of tracer in porcine myocardium at two sites where MSCs transfected with HSV-tk were injected 8 h earlier. **g** An example of hybrid ^{18}F-FHBG PET/CT imaging from the same study confirmed the localisation of injected cells in the anterior

left ventricular wall (both images are adapted with permission from [122]). *CMV* cytomegalovirus, *HSV-tk* herpes simplex virus thymidine kinase, *SPIO* superparamagnetic iron oxide, *^{18}F-FHBG(P)* 9-(4-^{18}F-fluoro-3-[hydroxymethyl] butyl)guanine (phosphate)

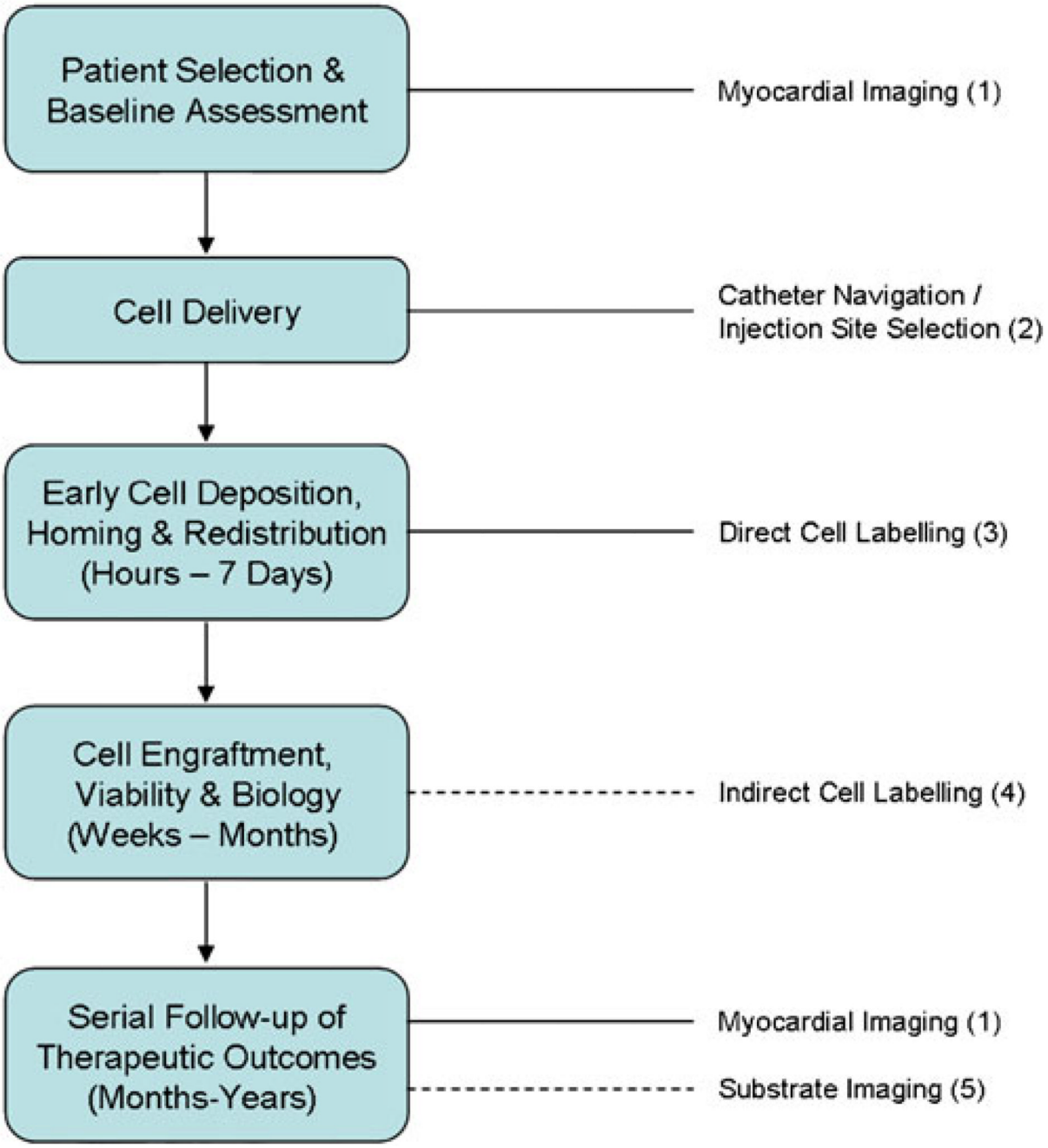

Fig. 3.

Integrated imaging of the cell therapy patient. This flow chart depicts the extensive and multifaceted applications for imaging in cardiac patients who receive cell therapy, spanning baseline evaluation and patient selection, the delivery procedure itself and the short- and long-term surveillance of cell fate, tissue substrate response and ultimately patient outcomes. Applicable imaging strategies: *1* MRI, SPECT, PET, echocardiography, left ventriculography for myocardial structure and function; coronary angiography and flow studies, myocardial stress imaging with SPECT, MRI or echocardiography for perfusion; late gadolinium enhancement MRI, PET for viability. *2* Biplanar X-ray fluoroscopy, electromechanical mapping, MRI fluoroscopy for guided cell delivery. *3* SPECT (e.g. ^{111}In),

PET (e.g. ^{18}FFDG, ^{64}Cu), MRI (e.g. SPIO) for short-term cell fate. *4* Reporter gene strategies and SPECT (e.g. sodium-iodide symporter), PET (e.g. HSV-*tk*), MRI (e.g. ferritin) for long-term cell fate. *5* Molecular imaging of cellular and myocardial targets (e.g. inflammation, apoptosis, angiogenesis). *Dotted lines* indicate that the imaging strategy has not yet been used clinically for its nominated purpose

Table 1

Clinical studies using image navigation for transendocardial cell delivery

Study authors (study name)	Catheter	Disease	Design	No. of patients	Cell type
(A) Electromechanical mapping					
Krause et al. [39]	MyoStar™	Acute MI	Non-controlled	20	BM MNC
Gyöngyösi et al. [155] (MYSTAR[a])	MyoStar™	Acute and chronic MI	Randomised time comparison	30 early, 30 late	BM MNC
Briguori et al. [156]	MyoStar™	Chronic IHD	Non-controlled	10	BM MNC
Beeres et al. [157]	MyoStar™	Chronic IHD	Non-controlled	25	BM MNC
Fuchs et al. [158]	MyoStar™	Chronic IHD	Non-controlled	27	BMC
Losordo et al. [11]	MyoStar™	Chronic IHD	RDBPCT dose-escalation	18 Rx, 6 placebo	G-CSF + $CD34^+$ cells
Tse et al. [159] (PROTECT-CAD)	MyoStar™	Chronic IHD	RBPCT dose-comparison	19 Rx, 9 placebo	BM MNC
van Ramshorst et al. [160]	MyoStar™	Chronic IHD	RDBPCT	25 Rx, 24 placebo	BM MNC
Perin et al. [38]	MyoStar™	Ischaemic CMP	NRCT	11 Rx, 9 control	BM MNC
Dib et al. [161] (CAuSMIC)	MyoStar™	Chronic MI/ischaemic CMP	RPCT dose-escalation	12 Rx, 11 placebo	SkM
(B) X-ray fluoroscopy					
Ince et al. [29]	MyoCath™	Chronic MI/ischaemic CMP	Case-controlled	6 Rx, 6 control	SkM
Smits et al. [30][b]	MyoStar™/MyoCath™	Chronic MI/ischaemic CMP	Non-controlled	15	SkM
de la Fuente et al. [31]	Helix™	Chronic MI/ischaemic CMP	Non-controlled	10	BM MNC
Duckers et al. [32] (SEISMIC)	MyoCath™	Ischaemic CMP	RCT	26 Rx, 14 control	SkM

BM bone marrow, *BMC* bone marrow cells, *CMP* cardiomyopathy, *G-CSF* granulocyte colony-stimulating factor, *IHD* ischaemic heart disease, *MI* myocardial infarct, *MNC* mononuclear cells, *(N)RCT* (non-)randomised controlled trial, *R(DB)PCT* randomised (double-blinded) placebo-controlled trial, *Rx* cell treatment, *SkM* skeletal myoblasts

MyoCath™ (Bioheart Inc., Sunrise, FL, USA) and Helix™ (Biocardia, Inc., South San Francisco, CA, USA)

[a] MYSTAR study compared timing of delivery for combined intramyocardial and intracoronary routes

[b] Both types of catheters were used in this study, with their respective imaging modality for navigation

Table 2

Clinical studies of cell labelling and tracking

Study	Disease	No. of patients	Cell type/ delivery route	Cell label	Imaging modality	Time	Results
Hofmann et al. [19]	Acute MI	3 (IC BMC), 3 (IV BMC), 3 (IC $CD34^+$)	Unf BMCs or $CD34^+$ cells/IC or IV	^{18}F-FDG	PET	50–75 min	Background signal only with IV. Augmented signal with $CD34^+$ cells. Signal in border ± MI zone
Kang et al. [67]	Acute MI	17 (IC), 3 (IV)	PB MNCs/IC or IV	^{18}F-FDG	PET/CT	2 h, 20 h (n=1)	No MI signal after IV. 1.5% retention in heart after IC
Silva et al. [64]	Acute MI	14 (IC), 10 (RICV), 6 (control)	BM MNCs/IC or RICV	^{99m}Tc-HMPAO	SPECT	4 h, 24 h	Retention higher with antegrade IC delivery route
Penicka et al. [65]	MI	5 (acute MI), 5 (chronic MI)	BM MNCs/IC	^{99m}Tc-HMPAO	SPECT	2 h, 20 h	Cardiac signal in 5/5 acute and 4/5 chronic patients at 2 h and in 3/5 acute and 0/5 chronic patients at 20 h
Schächinger et al. [109]	MI	8 (acute MI), 4 (inter MI), 5 (chronic MI)	PB MNCs/IC	^{111}In-oxine	Whole-body scintigraphy	1 h, 24 h, 3–4 days	Signal highest after 1 h and in acute MI group
Goussetis et al. [66]	Chronic MI/ischaemic CMP	8	BM $CD133^+$ or $CD34^+$ cells/IC	^{99m}Tc-HMPAO	SPECT	1 h (n=8), 24 h (n=4)	Cardiac retention 9.2% at 1 h and 6.8% at 24 h. Extracardiac signal in spleen and liver
Dedobbeleer et al. [108]	Chronic MI	7	PB $CD34^+$ cells/IC	^{18}F-FDG	PET/CT	1 h	3.2% retention at MI borders. Higher signal in liver, spleen, BM

All of the above studies involved direct cell labelling with radionuclide labels. Time column indicates the time after cell delivery that imaging was performed

CT computed tomography, *IC* intracoronary, *inter* intermediate aged, *IV* intravenous, *PB* peripheral blood, *PET* positron emission tomography, *RICV* retrograde intracoronary vein, *SPECT* single photon emission computed tomography, *Unf* unfractionated, *18F-FDG* ^{18}F-fluorodeoxyglucose, *99mTc-HMPAO* ^{99m}Tc-hexamethylpropylenamineoxine. Other abbreviations are defined in Table 1

Table 3

Comparison of imaging modalities for cell tracking

Monitoring strategy	Spatial resolution	Cell detection sensitivity
Direct labelling		
SPECT	++/+++	+++
PET	++/+++	+++
MRI	++++	++
Indirect labelling (reporter genes)		
SPECT	++/+++	+++
PET	++/+++	+++
MRI	++++	Unknown

Comparison of the spatial resolution and cell detection sensitivity of the three main imaging modalities that are translatable to cell tracking in clinical practice. Scale is semi-quantitative: + (least) to ++++ (most)

MRI magnetic resonance imaging, *PET* positron emission tomography, *SPECT* single photon emission computed tomography